

# A national data-based energy modelling to identify optimal heat storage capacity to support heating electrification

Jesus Lizana<sup>a,\*</sup>, Claire E. Halloran<sup>a</sup>, Scot Wheeler<sup>a</sup>, Nabil Amghar<sup>b</sup>, Renaldi Renaldi<sup>a,c</sup>, Markus Killendahl<sup>d</sup>, Luis A. Perez-Maqueda<sup>b</sup>, Malcolm McCulloch<sup>a</sup>, Ricardo Chacartegui<sup>e</sup>

<sup>a</sup> Department of Engineering Science, University of Oxford, Parks Road, Oxford, OX1 3PJ, United Kingdom

<sup>b</sup> Instituto de Ciencia de Materiales de Sevilla, Consejo Superior de Investigaciones Científicas – Universidad de Sevilla, Calle Américo Vespucio 49, 41092, Seville, Spain

<sup>c</sup> School of Water, Energy and Environment, Cranfield University, Cranfield, MK43 0AL, United Kingdom

<sup>d</sup> Tomorrow, Godthåbsvej 61, 2000, Frederiksberg, Denmark

<sup>e</sup> Departamento de Ingeniería Energética, Universidad de Sevilla, Camino de Los Descubrimientos S/n, 41092, Seville, Spain

## ARTICLE INFO

### Keywords:

Thermal energy storage  
Energy flexibility  
Heating  
Demand-side response  
Heat pump  
Heating decarbonisation

## ABSTRACT

Heating decarbonisation through electrification is a difficult challenge due to the considerable increase in peak power demand. This research proposes a novel modelling approach that utilises easily accessible national-level data to identify the required heat storage volume in buildings to decrease peak power demand and maximises carbon reductions associated with electrified heating technologies through smart demand-side response. The approach assesses the optimal shifting of heat pump operation to meet thermal heating demand according to different heat storage capacities in buildings, which are defined in relation to the time (in hours) in which the heating demand can be provided directly from the heat battery, without heat pump operation. Ten scenarios (S) are analysed: two baselines (S1–S2) and eight load shifting strategies (S3–S10) based on hourly and daily demand-side responses. Moreover, they are compared with a reference scenario (S0), with heating currently based on fossil fuels. The approach was demonstrated in two different regions, Spain and the United Kingdom. The optimal heat storage capacity was found on the order of 12 and 24 h of heating demand in both countries, reducing additional power capacity by 30–37% and 40–46%, respectively. However, the environmental benefits of heat storage alternatives were similar to the baseline scenario due to higher energy consumption and marginal power generation based on fossil fuels. It was also found that load shifting capability below 4 h presents limited benefits, reducing additional power capacity by 10% at the national scale. The results highlight the importance of integrated heat storage technologies with the electrification of heat in highly gas-dependent regions. They can mitigate the need for an additional fossil-based dispatchable generation to meet high peak demand. The modelling approach provides a high-level strategy with regional specificity that, due to common datasets, can be easily replicated globally. For reproducibility, the code base and datasets are found on GitHub.

## 1. Introduction

In-home thermal energy storage (TES) solutions can support the rapid decarbonisation of the domestic heating sector if correctly integrated with energy-efficient buildings and electrified heating technologies. This work deals with the problem of assessing, country by country, the optimal thermal storage capacity to support smart demand-side response (DR) in heating electrification. The aim is to reduce the required national power capacity while mitigating carbon emissions. An energy modelling approach using widely available data of heating

demand, electricity generation and associated carbon emissions is presented, which evaluates thermal load shifting strategies in the context of a country's electricity generation mix and heating electrification effort.

The complete decarbonisation of the domestic space and water heating sector is extremely challenging but a requirement in the global effort to mitigate greenhouse gas (GHG) emissions [1,2]. A promising solution toward a future low-carbon heating sector is energy-efficient buildings with thermal energy storage (TES) solutions integrated with electrified low-carbon technologies such as heat pumps (HPs) [3,4]. However, in the long term, the decarbonisation of heat through electrification needs to be coupled with the successful decarbonisation of the

\* Corresponding author.

E-mail address: [jesus.lizana@eng.ox.ac.uk](mailto:jesus.lizana@eng.ox.ac.uk) (J. Lizana).

<https://doi.org/10.1016/j.energy.2022.125298>

Received 25 December 2021; Received in revised form 3 July 2022; Accepted 24 August 2022

Available online 5 September 2022

0360-5442/© 2022 The Authors. Published by Elsevier Ltd. This is an open access article under the CC BY license (<http://creativecommons.org/licenses/by/4.0/>).

| Nomenclature                  |   |
|-------------------------------|---|
| BCI                           | hourly average baseline carbon intensity rate, $\text{gCO}_{2\text{eq}}/\text{kWh}$ |
| cc                            | maximum heating capacity constraint, MW   |
| CI                            | hourly average carbon intensity rate, $\text{gCO}_{2\text{eq}}/\text{kWh}$          |
| COP                           | coefficient of performance  |
| DHC                           | district heating and cooling  |
| DR                            | demand-side response  |
| $DR_s$                        | hourly demand response pattern per scenario   |
| DSM                           | demand-side management  |
| EC                            | baseline of power consumption per hour, MW  |
| EF                            | improvement in energy efficiency, %   |
| f                             | fraction of annual non-renewable heating demand                                     |
| FEC                           | final energy consumption, MW  |
| GHG                           | greenhouse gas  |
| $GHG_s$                       | total carbon emissions per scenario, Mtonnes $\text{gCO}_{2\text{eq}}$              |
| $\text{grid}_{\text{factor}}$ | average transmission and distribution losses  |
| HD                            | thermal heating demand, GWh   |
| HDD                           | heating degree days   |
| HP                            | heat pump   |
| IPCC                          | Intergovernmental Panel on Climate Change   |
| LOAD                          | hourly electricity power demand, MW   |
| m                             | multiplier to normalised heating demand   |
| MCI                           | hourly average marginal carbon intensity rate, $\text{gCO}_{2\text{eq}}/\text{kWh}$ |
| S                             | scenario  |
| sCOP                          | seasonal coefficient of performance   |
| sf                            | shape factor to balance heating demand below cc                                     |
| TABS                          | thermally activated buildings systems   |
| $T_{\text{eff}}$              | typical efficiencies of heating technologies  |
| TES                           | thermal energy storage  |
| TESC                          | thermal energy storage capacity in time per scenario, hours                         |
| $TES_{\text{losses}}$         | increase in energy consumption due to thermal losses, %                             |
| UCI                           | hourly average updated carbon intensity rate, $\text{gCO}_{2\text{eq}}/\text{kWh}$  |
| UK                            | United Kingdom  |
| V2G                           | vehicle-to-grid   |
| WIND                          | additional wind power generation per hour, MW                                       |
| <i>Subscript</i>              |   |
| h                             | hour  |
| i                             | heating sector: space heating (sh) or hot water (w)                                 |
| s                             | scenario  |
| sh                            | space heating   |
| w                             | hot water   |

electricity grid [5,6], which makes it more challenging [7]. Depending on the heating technologies deployed and the degree of consumer behavioural change, a significant increase in peak power demand might be observed. These peaks may not align well with renewable generation such as solar and wind which may cause significant adverse consequences on carbon emissions in the short term, increasing peak power generation capacity from fossil fuel sources. The distributed nature of electrification is also likely to put low-voltage distribution networks that deliver power from the substations to end-users through residential streets, underer significant strain [8].

Heating electrification's impact has been previously studied nationally, with important implications in highly gas-dependent regions. Borge-Diez et al. [9] compared HPs and natural gas boilers for heating and concluded that the projected cost of HPs may be cheaper. The study showed that 90% of Spain can be covered with this approach by 2050. Love et al. [10] evaluated an aggregated load profile using data from 696 heat pumps in Great Britain. They found that peak grid demand may increase by 7.5 GW (14%), with 20% of households installing heat pumps. Watson et al. [11] predicted peak domestic heat demand in Great Britain ranged from 159 GW to 170 GW depending on the annual ambient temperature. In an updated study, they reported a potential peak heat demand of 157 GW [12].

Energy flexibility, in a variety of forms, is being widely investigated to help accommodate demand growth and variable renewable generation on low-carbon electricity networks [13–17]. Integrated TES solutions and flexible buildings using smart DR may offer more efficient and accessible alternatives to home batteries or vehicle-to-grid (V2G) [18–20]. Thermal batteries are claimed to be 60–90% cheaper, being a much more cost-effective solution for providing energy for heat than the cheapest Li-ion alternative [3]. The opportunity for flexible energy systems based on heat storage to support heating electrification is moving rapidly through global energy policy discourse [3]. Lizana et al. [21] demonstrated how energy flexible buildings could support the network by efficiently shifting heat consumption to off-peak hours, achieving economic savings of 20% for end-users and 25% for retailer's associated electricity costs due to the advantage of cheaper and low-carbon energy generation technologies. Several studies have identified electricity system benefits from heat storage, including reduced wind curtailment and lower generation capacity requirements for heat electrification [22–24]. Moreover, to support electricity

decarbonisation, the ElectricityMap project, built by Tomorrow [25], provides access to real-time data from power generation and associated carbon intensities around the world [26], along with the short-term forecasting of hourly average marginal carbon intensity values [27]. This data can support load shifting towards lower carbon intensity periods. However, most of the previous studies on heating flexibility specifically focus on specific building cases or clusters of buildings, not considering the implications of heat batteries for load aggregation at the national level [28]. The optimal thermal storage capacity in flexible heating to maximise carbon reductions without dramatically increasing power capacity is highly dependent on the heating demand volume per country, existing electricity demand profile and available generation technologies. These optimal heat storage alternatives may differ by country and should be promoted explicitly through future regulations toward efficient and low-carbon heating electrification. There is a need to understand the implications of heat storage on load aggregation following energy flexibility strategies to shape sustainable power systems based on renewable energy sources.

This work proposes a novel top-down energy modelling approach that utilises easily accessible national-level data to analyse the implications of in-home heat batteries on heating electrification following energy flexibility strategies. The aim is to identify the optimal TES capacity for DR in electrified heating technologies per region that minimises additional power capacity while maximising carbon reductions, which should be promoted in new residential heating technologies. The approach assesses the optimal shifting of heat pump operation according to different heat storage capacities. These TES capacities are defined in relation to the time (in hours) in which the heating demand can be provided directly from the heat battery, without heat pump operation. The novelty is based on top-down national energy modelling of different smart DR response alternatives using easily accessible national-level data on heating demand, power generation and associated carbon emissions. The approach can be easily applied to other regions making direct comparisons possible.

The model scope is limited to the residential sector and short-term targets since it is based on the existing performance of the electricity grid and residential heating demand patterns. In this study, the short-term electrification target was defined as 10% of existing non-renewable residential final energy consumption (FEC) of heating per country, according to Eurostat [29]. This fraction involves current FEC

for heating based on solid fossil fuels, natural gas and oil and petroleum products.

Two baseline scenarios without heat storage were defined. One involves direct heating electrification (scenario S1), and another consists of heating electrification with demand reduction by 20% due to improvements in energy efficiency in buildings (S2). Next, eight load shifting scenarios for heating electrification through different hourly and daily DR strategies were evaluated through a parametric analysis. They also involve a heating demand reduction of 20%. Moreover, they are compared with a reference scenario (S0), with heating currently based on fossil fuels.

The top-down modelling approach is divided into five steps: (1) Calculation of hourly heating demand; (2) Definition of demand scenarios with and without smart DR; (3) Definition of projected grid scenario related to expected renewable generation; (4) determination of additional electricity load per demand scenario; and (5) calculation of GHG emissions. The method was tested and demonstrated in two regions, Spain and the United Kingdom (UK). These regions were selected in order to compare heat storage implications for heating electrification in two contexts characterised by different electricity demand profiles, generation technologies and heating needs. The renewable power generation mix in the UK's electricity grid was responsible for 24.4% in 2018, while it was 37.2% in Spain. The non-renewable heating sector of households is responsible for 19.4% of total FEC in the UK, while it only represents 6% in Spain [29].

The paper is structured as follows. Data sources and methods are described in section 2. The results and discussion are detailed in section 3, divided into four subsections: analysis of input data, analysis of output results, policy implications, and limitations of the study. Finally, conclusions are presented.

## 2. Data and methods

A schematic diagram of the top-down energy modelling using national data to evaluate the implications of heat storage for heating electrification is provided in Fig. 1. It illustrates the input data and methods defined in the analysis. Input data per country are obtained from four different databases: Eurostat open dataset (A), International Energy Agency (B), Data Platform: When2Heat (C), and ElectricityMap database (D). The approach is divided into five steps: heating demand (1), demand scenarios (2), grid scenario (3), electricity load (4), and GHG emissions (5). The approach was developed using Python. The source code and datasets are published on GitHub (<https://github.com/lizanafj/national-data-based-energy-modelling>) together with additional documentation. Data and methods are described in detail in sections 2.1 and 2.2, respectively.

This modelling approach can support the decision-making process for short-term residential electrification targets on a national scale since it is based on real national data regarding heating demand patterns and electricity generation. The method was demonstrated in two countries, Spain and the UK, using data for 2018 and 2019. However, the approach is designed to be broadly applicable to countries across Europe according to data available in selected open-access databases.

### 2.1. Data per country

This section describes the four databases and the specific input data required for the analysis, previously summarised in Fig. 1.

The Eurostat open dataset [29] provides data on annual non-renewable FEC of heating demand for space heating and hot water per country. These data were also complemented with national data, where available, such as those reported by the government of the UK [30]. Two years were selected for the analysis, 2018 and 2019, before the COVID-19 pandemic. Extracted and reassembled data were contrasted with existing reports [31,32] to ensure an accurate data selection. Additionally, average heating degree days (HDDs) per country

were extracted to convert the annual heating demand for space heating into a monthly distribution.

Data provided by the International Energy Agency [5] regarding typical efficiencies ( $T_{eff}$ ) of heating technologies are used to calculate annual thermal heating demand using non-renewable FEC of heating per country. They are summarised in Table 1.

The When2Heat dataset [33–35] is used to define hourly heat demand patterns to increase the resolution of monthly data into hourly demand. This dataset includes simulated hourly country-aggregated heat demand and coefficient of performance (COP) time series for 28 European countries. Heat demand is calculated based on standard gas load profiles and reanalysis data of temperature and wind speed. Spatial heat demand is aggregated for each country using population-weighting and scaled to final national energy consumption for heating from the EU Building Database. COP values are calculated based on reanalysis data of temperature and wind speed and manufacturer data, then aggregated to national-level values based on heat demand. These data are used to define average annual normalised hourly residential space and water heating demand profiles, as shown in Fig. 2, and seasonal COP values of space heating and hot water cycles for each month per country, as shown in Fig. 3. The COP value for an air-source heat pump with radiators is used for space heating since this is the most common configuration in Spain and the UK [10,36]. It can be appreciated how normalised residential demand profiles (Fig. 2) are similar (not identical), perhaps due to similar lifestyle habits, while the seasonal COP (Fig. 3) is affected by average climate conditions per region.

ElectricityMap database [25] was used to obtain operational data for the electricity system, in this case for Spain and the UK. Electricity Map collects real-time data from power generation and imports/exports worldwide. Datasets for the same period, 2018 and 2019, were used with an hourly resolution, containing data associated with power production, power consumption, average carbon intensity and average marginal carbon intensity rates, among others. The input data selected are summarised in Table 2.

Power consumption refers to the total hourly power consumed per region (in MW), involving production and imports by generation technology. Power production is associated with the hourly power production per region (in MW), which differs from consumption since it doesn't include imports. Also, production excludes storage or discharge.

Hourly average carbon intensity ( $gCO_{2eq}/kWh$ ) provided by ElectricityMap [25] was calculated considering hourly power consumption by generation technology (including imports) and using carbon emission intensities per generation technology derived from IPCC 2014 [37,38], detailed in Table 3. They are based on the global warming potential unit (carbon dioxide equivalent,  $kgCO_{2eq}$ ) per kilowatt-hour (kWh). These emissions include the entire lifecycle of the generation technology, from material and fuel mining through construction to operation and waste management. Further details on country-specific values are provided in the GitHub repository [39].

Hourly marginal carbon emission intensity ( $gCO_{2eq}/kWh$ ) provided by ElectricityMap [25] was calculated using a machine learning regression algorithm on historical load and generation data per country [40]. Flow tracing of marginal electricity sources from in-country generation and cross-border imports is used to create a marginal topology matrix of the fractional sources of a marginal unit of electricity consumed in each country for every hour of historical data. Historical data was also used to infer the marginal generation types for each country, and marginal generation emissions were estimated based on generation types and shares. Finally, each country's marginal emissions of power consumption were calculated as the average of generation emissions from each marginal generation country, weighted by the share of marginal electricity from each country.

### 2.2. Methods: a top-down energy modelling using national data

The performance of TES in buildings at a national scale to support

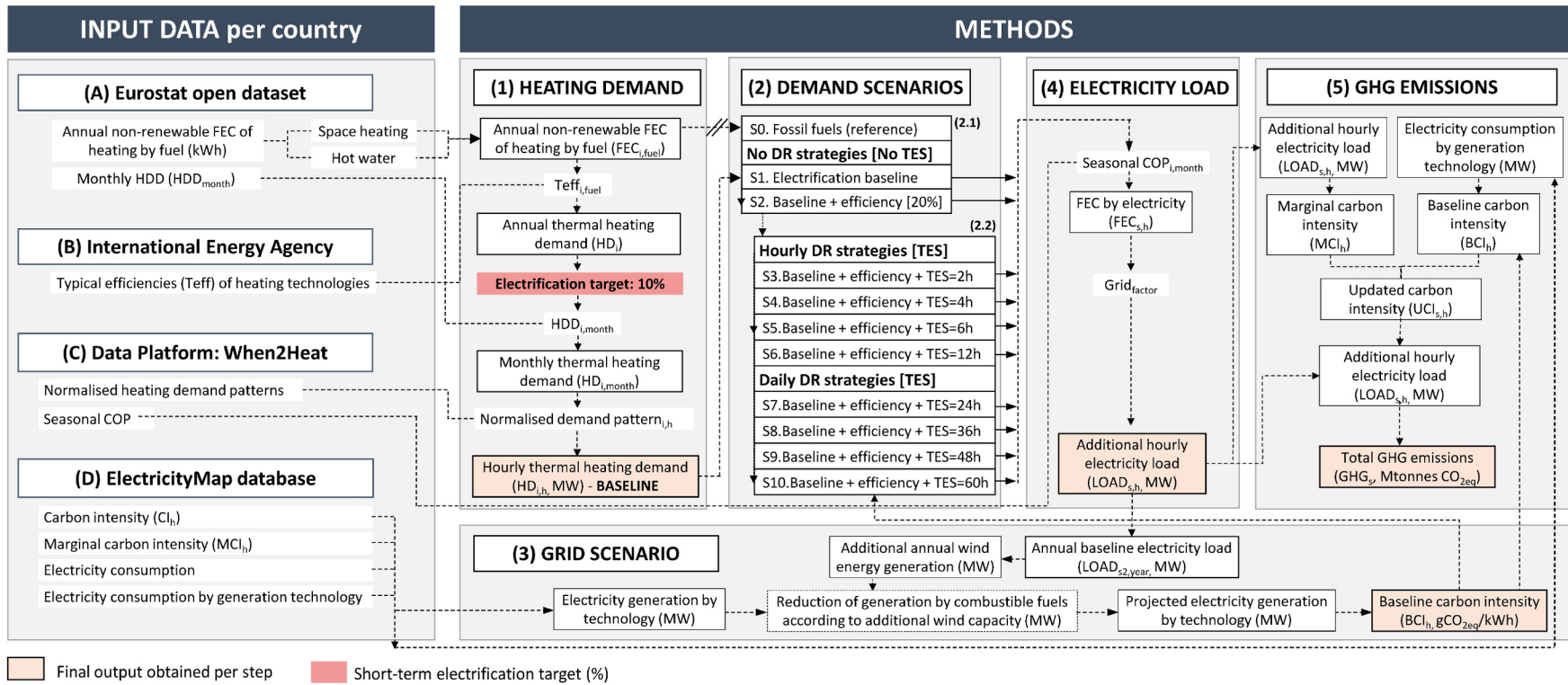


Fig. 1. Schematic diagram of workflow explaining the top-down energy modelling using national data to evaluate the implications of heat storage for heating electrification.

**Table 1**  
Typical efficiencies ( $T_{eff}$ ) of heating technologies. Data source: IEA [5].

| Heating technology            | Efficiency ( $T_{eff}$ ) | Fuels                |
|-------------------------------|--------------------------|----------------------|
| Conventional boilers/furnaces | 0.60–0.84                | Oil, natural gas     |
| Condensing boilers            | 0.85–0.97                | Oil, natural gas     |
| Wood stoves/furnaces          | <0.70                    | Biomass              |
| High-efficiency fireplaces    | 0.70–0.80                | Biomass, natural gas |
| Heat pumps (electric)         | 2.0–6.0                  | Electricity          |

heating electrification and decarbonisation is evaluated through five steps, previously illustrated in Fig. 1: (1) Calculation of hourly heating demand; (2) definition of demand scenarios with and without smart DR; (3) definition of projected grid scenario related to expected renewable

generation; (4) determination of additional electricity load per demand scenario; and (5) calculation of GHG emissions. Further details of the process are detailed below.

2.2.1. Calculating hourly heating demand

Thermal heating demand ( $HD_i$ ) for electrification per country, involving space heating and hot water demand, was defined as a short-term reference target of 10% of current annual non-renewable FEC for heating in households. This FEC target value was obtained from the Eurostat open database [29], considering heating associated with solid fossil fuels, natural gas and oil and petroleum products [29,30].

Firstly, the annual thermal heating demand per space heating and hot water ( $HD_i$ , MWh) was calculated according to Eq. (1), considering typical efficiencies of heating technologies by fuel, as defined in Table 1

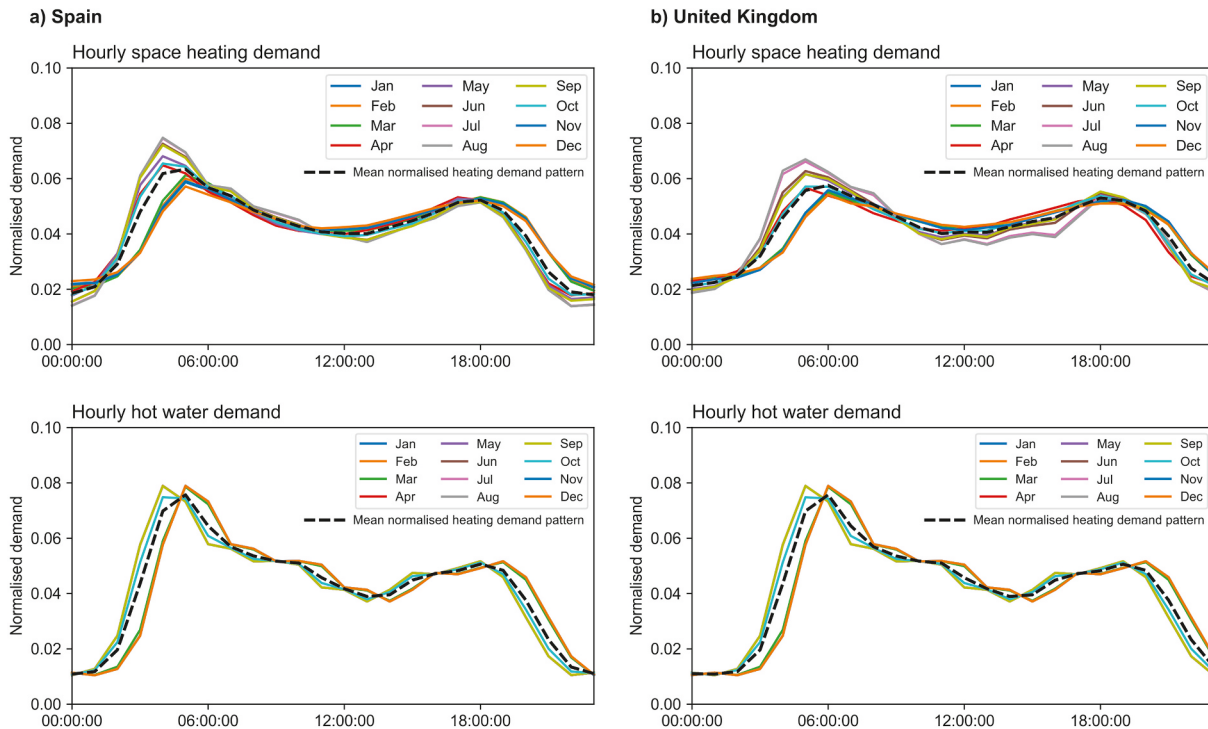


Fig. 2. Normalised heating demand patterns for space and water heating for Spain (a) and the UK (b), based on the When2Heat dataset.

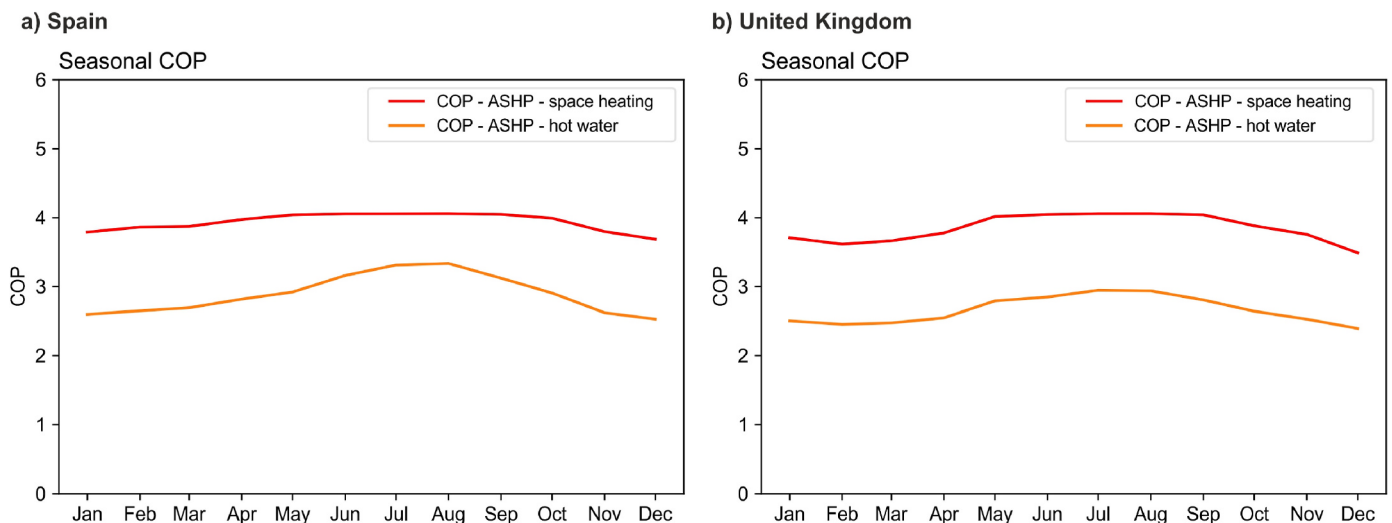


Fig. 3. Monthly COP values for space heating with an air-source heat pump and radiator (red line); and for hot water heating with an air-source heat pump (orange line) for Spain (a) and the UK (b), based on the When2Heat dataset.

**Table 2**  
Main indicators of ElectricityMap database used.

| Indicator                                  | Units                   | Nomenclature in ElectricityMap <sup>a</sup> | Description  |
|--|-------------------------|---|--|
| Power consumption                          | MW                      | power_consumption_avg                       | Production + Discharge + Import - Export - Storage                                       |
| Power consumption by generation technology | MW                      | power_consumption_source_avg                | Associated with consumption, which considers imports                                     |
| Percentage of renewables <sup>b</sup>      | %                       | power_origin_percent_renewable_avg          | In consumption   |
| Power production                           | MW                      | power_production_avg                        | Production excludes storage or discharge   |
| Power production by generation technology  | MW                      | power_production_source_avg                 |  |
| Percentage of renewables                   | %                       | power_production_percent_renewable_avg      | In production  |
| Average carbon intensity                   | gCO <sub>2</sub> eq/kWh | carbon_intensity_avg                        | Average carbon intensity associated with total consumption, which considers imports      |
| Average marginal carbon intensity          | gCO <sub>2</sub> eq/kWh | marginal_carbon_intensity_avg               | Average marginal carbon intensity associated with the marginal power for additional load |

<sup>a</sup> Default nomenclature used in the ElectricityMap database.

<sup>b</sup> Renewables include hydro, wind, solar, biomass and geothermal energy.

**Table 3**  
CO<sub>2</sub>-eq intensity per generation technology.

| Origin            | Technology        | Carbon intensity (gCO <sub>2</sub> eq/kWh) <sup>a</sup> |
|-------------------|-------------------|---|
| Renewables        | Solar             | 45  |
|                   | Geothermal        | 38  |
|                   | Wind              | 11  |
|                   | Hydro             | 24  |
|                   | Biomass           | 230   |
| Storage           | Battery discharge | 301   |
|                   | Hydro discharge   | 301   |
| Nuclear           | Nuclear           | 12  |
| Combustible fuels | Gas               | 490   |
|                   | Oil               | 650   |
|                   | Coal              | 820   |
|                   | Unknown           | 700   |

<sup>a</sup> Average carbon intensity, including the whole life of the source, is derived from IPCC 2014 [37,38].

by the IEA [5] (section 2.1).

$$HD_i = \sum_{fuel}^n FEC_{i,fuel} \cdot T_{eff,i,fuel} \quad (1)$$

where:

$HD_i$ : annual thermal heating demand (GWh/year).

$i$ : space heating (sh) or hot water (w).

$FEC_{i,fuel}$ : final energy consumption per fuel in GWh according to Eurostat [29].

$T_{eff,i,fuel}$ : Typical efficiency for heating technologies by fuel, reported in Table 1.

Secondly, monthly thermal heating demand values ( $HD_{i,month}$ , MWh) were obtained according to Eq. (2), which considers a constant distribution throughout the year for hot water demand, while monthly space heating demand was calculated according to the monthly fraction of heating degree days (HDD) reported by Eurostat [29]. In this step, the electrification target ( $f$ ) for non-renewable heating is implemented, previously defined as 10%.

$$HD_{sh, month} = f \cdot 1000 \cdot \left( HD_{sh} \frac{HDD_{month}}{HDD_{total}} \right)$$

$$HD_{w, month} = f \cdot 1000 \cdot \left( HD_w \frac{1}{12} \right) \quad (2)$$

where:

$HD_{sh}$ : annual thermal heating demand for space heating.

$HD_w$ : annual thermal heating demand for water heating.

$HD_{sh, month}$ : monthly thermal heating demand for space heating (MWh/

month).

$HD_{w, month}$ : monthly thermal heating demand for hot water (MWh/month).

$HDD_{total}$ : heating degree days per year.

$HDD_{month}$ : heating degree days per month.

$f$ : fraction of annual non-renewable heating demand for the analysis (defined as 10% of current FEC for heating based on fossil fuels).

Finally, once monthly values were determined, they were resampled in an hourly frequency using normalised heating demand profiles for space heating and hot water, separately, according to Eq. (3). Normalised demand patterns were explicitly obtained per country from When2Heat dataset [33–35].

$$HD_{i,h} = \frac{HD_{i, month}}{Days_{month}} \cdot Pattern_{i,h} \quad (3)$$

where:

$HD_{i,h}$ : hourly thermal heating demand (MW/hour).

$i$ : space heating (sh) or hot water (w).

$HD_{i, month}$ : monthly thermal heating demand (MWh/month).

$Days_{month}$ : number of days per month.

$Pattern_{i,h}$ : normalised heating demand pattern.

This approach makes the method widely applicable to other regions by lowering the input data required to those widely available in existing databases.

### 2.2.2. Definition of demand scenarios

This method evaluates heat demand for heating electrification through a parametric analysis of ten scenarios. The scenarios, which are summarised in Table 4, are obtained in the two-stage process described below.

The first stage (2.1 in Fig. 1) defines the baseline for heating electrification with no TES. It involves two scenarios (S1 and S2). S1 consists of a direct electrification baseline where electricity is consumed according to heating demand, while S2 includes improvements in the energy efficiency of buildings in order to reduce heating demand by 20%. This S2 demand scenario is used as a reference demand for next scenarios (from S3 to S10), and in section 2.3.3 to define the projected renewable generation capacity.

The second stage (2.2 in Fig. 1) evaluates heating demand alternatives by implementing TES and DR. Scenarios are grouped into shifting strategies with TES for hourly DR (S3–S6) and TES for daily DR (S7–S10). Hourly DR scenarios (S3–S6) use a heat storage capacity ranging from 2 to 12 h. Daily DR scenarios (S7–S10) simulate heating electrification using a heat storage capacity ranging from 1 to 2.5 days of thermal heating needs. In these scenarios, heating demand is evaluated from the point of view of electricity load, not the supply of thermal heating to the users. Thus, HP operation is shifted per scenario according to implemented TES capacity to store the required heat to meet reference heating demand (demand of S2), and the operation period is mainly

**Table 4**  
Demand scenarios for heating electrification.

| Scenarios                                  | TES capacity <sup>a</sup> (demand in hours) | Maximum heating capacity constraint (cc, MW) | Energy consumption increase <sup>b</sup> (%) |
|--|---|--|--|
| S0. Fossil fuels (reference)               | –   | –  | –  |
| <b>No DR strategies</b>                    |   |  |  |
| S1. Baseline                               | –   | –  | –  |
| S2. Baseline +20% efficiency               | –   | –  | –  |
| <b>Hourly DR strategies</b>                |   |  |  |
| S3. Baseline +20% efficiency + TES (2 h)   | 2 h   | $\max(S1) \cdot 0.70$                        | +1.0%  |
| S4. Baseline +20% efficiency + TES (4 h)   | 4 h   | $\max(S1) \cdot 0.75$                        | +1.5%  |
| S5. Baseline +20% efficiency + TES (6 h)   | 6 h   | $\max(S1) \cdot 0.80$                        | +2.0%  |
| S6. Baseline +20% efficiency + TES (12 h)  | 12 h  | $\max(S1) \cdot 1.00$                        | +4.0%  |
| <b>Daily DR strategies</b>                 |   |  |  |
| S7. Baseline +20% efficiency + TES (24 h)  | 1 day                                       | $\max(S1) \cdot 1.05$                        | +8.0%  |
| S8. Baseline +20% efficiency + TES (36 h)  | 1.5 days                                    | $\max(S1) \cdot 1.05$                        | +12.0%                                       |
| S9. Baseline +20% efficiency + TES (48 h)  | 2 days                                      | $\max(S1) \cdot 1.10$                        | +15.0%                                       |
| S10. Baseline +20% efficiency + TES (60 h) | 2.5 days                                    | $\max(S1) \cdot 1.10$                        | +18.0%                                       |

<sup>a</sup> TES capacity in hours represents the period when thermal heating supply can be directly obtained from the heat battery without HP operation.

<sup>b</sup> The increase in energy consumption is related to the thermal losses during the thermal energy storage period.

increased according to heat losses during heat storage periods.

All proposed scenarios were also compared with a reference scenario S0, representing the current GHG emissions of the heating demand volume evaluated based on the 10% of FEC for residential heating currently supplied by fossil fuels.

TES alternatives are characterised by considering the different TES available technologies for buildings [41], summarised in Fig. 4. The shifting capacity of heating demand can be configured through different TES applications such as increasing building heat storage capacity (thermal inertial), implementing thermally activated buildings systems (TABS), heat storage components in ventilation systems, or heat batteries in the form of tanks. According to hourly or daily heating needs, these different TES applications can be specifically designed and combined to meet the timeframe in which thermal heating supply should be directly obtained from the heat battery without HP operation.

To evaluate the DR scenarios through different TES alternatives, the following assumptions are made:

- (a1) The heat storage capacity per scenario is defined by time, meaning the period in hours that thermal heating supply can be directly obtained from the heat battery without power consumption for HP operation. This assumption makes the model results widely scalable to different building sizes.
- (a2) All scenarios have constraints associated with the maximum heating capacity (defined in Table 4), assuming that a similar heat pump size to the baseline scenario (S1) would be used. These constraints ensure that the shifting of HP operation never increases peak power demand for hourly DR strategies, limiting

shifting capacity between 70 and 80% of HP capacity in these scenarios; and maximise shifting capacity for daily DR strategies assuming a moderate capacity increase by up to 10%.

- (a3) FEC of heating electrification using TES is increased in order to consider thermal losses during the thermal storage period. The values used are detailed in Table 4, according to data reported by previous studies [21,41–44].

Eq. (4) is proposed to evaluate the hourly heating demand per DR scenario with TES. It consists of an iterative rule-based process as a function of the heat storage capacity in time (hours), hourly average baseline carbon intensity rate ( $BCI_h$ ) as a penalty signal, maximum heating capacity according to baseline capacity in S1, and thermal losses ( $TES_{losses}$ ). The system balances thermal heating demand per scenario according to the proposed TES capacity, ensuring that the maximum hourly heating capacity is below the defined constraint and total flexible heating consumption is equal to the projected heating demand. Eq. (4.1) defines the demand pattern according to lower BCI rates and existing demand patterns. Eqs. (4.2), (4.3) and (4.4) normalise the defined demand pattern according to existing heating demand, and increment heating consumption according to TES losses ( $TES_{losses,s}$ ) during storage periods. Eq. (4.5) calculates total heating demand according to the defined demand pattern ( $HD_{s,h}$ ). Finally, after every iteration, the shape factor (sf) is increased by 0.001 in order to decrease the maximum heating capacity of the system. If  $\max(HD_{s,h})$  is still higher than  $\max(HD_{s1,h})-cc$ , the loop starts again, increasing sf by 0.001.

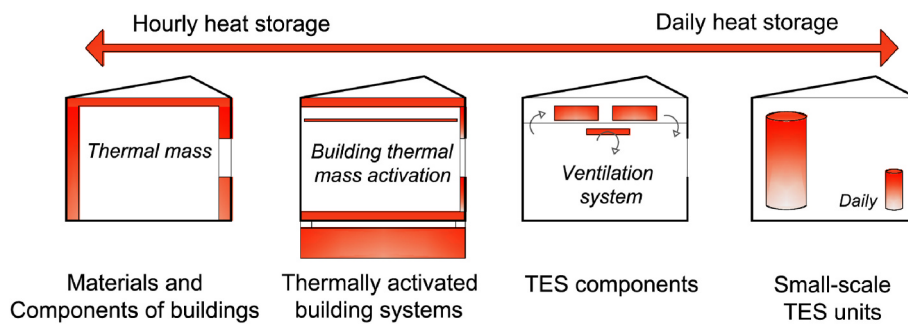


**Fig. 4.** Heat storage alternatives in buildings for hourly and daily DR strategies in heating electrification.

$$sf = 0$$

while  $\max(HDs, h) > \max(HDs1, h) \cdot cc :$

$$(4.1) DR_{s,i,h} = \begin{cases} 1 & \text{if } BCI_h < 50^{th} \text{ percentile every } TESCs \\ sf \cdot Pattern_{i,h} & \text{otherwise} \end{cases}$$

$$(4.2) HD_{s,i,h} = \frac{HD_{i,month} \cdot EF}{Days_{month}} \cdot DR_{s,i,h}$$

$$(4.3) m = \frac{\sum HD_{s2,i,h}}{\sum HD_{s,i,h}}$$

$$(4.4) HD_{s,i,h} = \frac{HD_{i,month} \cdot EF}{Days_{month}} \cdot DR_{s,i,h} \cdot m \cdot TES_{losses,s} \quad (4)$$

$$(4.5) HD_{s,h} = HD_{s,sh,h} + HD_{s,w,h}$$

$$(4.6) sf = sf + 0.001$$

where:

*sf*: shape factor to balance heating demand below maximum heating capacity.

*HD<sub>s,h</sub>*: hourly thermal heating demand per scenario (s) (MW).

*cc*: Maximum heating capacity constraint as a function of baseline capacity in S1, defined in Table 4.

*DR<sub>s,i,h</sub>*: hourly demand response pattern.

*BCI<sub>h</sub>*: hourly average baseline carbon intensity rate (gCO<sub>2</sub>eq/kWh).

*TESCs*: thermal energy storage capacity in time (hours) per scenario.

*Pattern<sub>i,h</sub>*: hourly normalised heating demand pattern.

*HD<sub>i,month</sub>*: monthly thermal heating demand (MWh/month).

*EF*: improvement in energy efficiency (default value = 20%)

*Days<sub>month</sub>*: number of days per month

*m*: multiplier to match total heating demand according to scenario S2.

*TES<sub>losses,s</sub>*: increase in heating demand associated with TES losses during storage periods, defined in Table 4.

*s*: scenario (from 1 to 10).

*i*: space heating (sh) or hot water (w).

### 2.2.3. Projected grid scenario related to expected renewable generation

This step defines the projected generation capacity by technology to evaluate the impact of different heating electrification scenarios. The analysis can be carried out considering the electricity network's existing generation and marginal capacity, or implementing expected scenarios for future generation technologies.

To obtain a reasonable short-term performance quantification, this work considers the projected renewable generation mix for a modest 10% heating electrification scenario. For the purposes of this study, the additional electricity load associated with heading is met through additional wind generation (WIND<sub>h</sub>) equated annually, according to Eq. (5). This additional wind capacity decreases the average carbon intensity of electricity by displacing combustible fuel generation at high wind times. This new hourly average carbon intensity is called average baseline carbon intensity (BCI<sub>h</sub>). For this small change in the generation mix, average marginal carbon intensity remains unchanged as we assume the marginal generation source remains the same. This is reasonable as the additional wind generation is never observed to result in the elimination of the existing marginal generation source within any given hourly period.

$$WIND_h = \frac{\sum_{h=0}^n LOAD_{s2,h}}{\sum_{h=0}^n PP_{wind,h}} \cdot PP_{wind,h} \quad (5)$$

where:

*WIND<sub>h</sub>*: Additional wind power generation per hour (MW).

*LOAD<sub>s2,h</sub>*: Hourly electricity power demand for heating electrification in scenario 2 per hour (MW).

*PP<sub>wind,h</sub>*: Existing power production by wind per hour (MW).

### 2.2.4. Hourly electricity load profile for each scenario

This step calculates the additional hourly electricity load profile (LOAD<sub>s,h</sub>, MW) according to the heat demand per scenario according to Eq. (6). It involves the calculation of final energy consumption (FEC<sub>s,h</sub>) associated with the electric power demand of HPs and average transmission and distribution losses (grid<sub>factor</sub>) [45]. As the evaluation is carried out at the country level, without data associated with the part-load operation and environmental operating conditions, only power under seasonal COP conditions of HPs was considered. Average monthly COP for space heating and hot water per country are used. They were obtained from the When2Heat dataset [33–35]. Transmission and distribution losses (grid<sub>factor</sub>) in the grid were assumed to be 5% [6].

$$LOAD_{s,h} = \frac{HD_{s,i,h}}{sCOP_{i,month}} \cdot grid_{factor}$$

$$LOAD_{s,h} = FEC_{s,hour} \cdot grid_{factor} \quad (6)$$

where:

*LOAD<sub>s,h</sub>*: Additional hourly electricity power demand per scenario per hour (MW).

*HD<sub>s,i,h</sub>*: hourly thermal heating demand per scenario (MW).

*sCOP<sub>i,month</sub>*: seasonal coefficient of performance.

*grid<sub>factor</sub>*: average transmission and distribution losses.

### 2.2.5. Calculating GHG emissions

Finally, GHG emissions per scenario (GHG<sub>s</sub>) were evaluated according to Eq. (7). It calculates the GHG emissions according to an updated average carbon intensity rate (UCI<sub>s,h</sub>) per scenario calculated according to Eq. (8). This updated average carbon intensity considers the average baseline carbon intensity rate per scenario (BCI<sub>s,h</sub>) according to the projected electricity generation defined in step 3 (section 2.3.3), and the average marginal carbon intensity in the grid (MCI<sub>h</sub>) for the additional load.

$$GHG_s = \sum_0^{h_h} LOAD_{s,h} \cdot 1000 \cdot UCI_{s,h} \quad (7)$$

$$UCI_{s,h} = \frac{EC_h \cdot BCI_h + LOAD_{s,h} \cdot MCI_{marginal,h}}{EC_h + LOAD_{s,h}} \quad (8)$$

where:

*GHG<sub>s</sub>*: total carbon emissions per scenario considering marginal power capacity for the aggregated load (gCO<sub>2</sub>eq).

*LOAD<sub>s,h</sub>*: additional hourly electricity power demand per scenario per hour (MW).

*UCI<sub>s,h</sub>*: hourly average updated carbon intensity of grid (gCO<sub>2</sub>eq/kWh) according to Eq. (8).

*EC<sub>h</sub>*: baseline of power consumption per hour (MW).

*BCI<sub>h</sub>*: hourly average baseline carbon intensity of grid (gCO<sub>2</sub>eq/kWh) obtained in section 2.3.3.

*MCI<sub>h</sub>*: hourly average marginal carbon intensity of grid associated with the marginal power capacity (gCO<sub>2</sub>eq/kWh).

## 3. Results and discussion

The results are shown and discussed in four subsections. First, input data are analysed in order to show the energy context of each simulated country. Second, the model results per country are compared and discussed. Third, potential policy implications are extracted. Finally, the limitations of the study are clarified.

### 3.1. Analysis of input data

#### 3.1.1. The heating sector per country

The space heating and hot water heating sector of households, from



hereon simply “heating sector”, was responsible for 20.5% of the total FEC of Europe in 2018 [29,32]. This heating demand varies between countries. Using data from Eurostat, the heating sector is responsible for 10.4% and 22.5% of total FEC in Spain and the UK, respectively [29], as illustrated in Fig. 5a and b.

Both case studies represent different baselines of the heating sector in Europe. In the case of Spain, only 6.0% of FEC is associated with non-renewable energy consumption for heating, while it represents 19.4% in the UK.

Fig. 5c shows the share of fossil fuels in the heating sector across Europe. The average share of fossil fuels in the heating sector for Europe as a whole was 56.5% in 2018, with Ireland (90%), Luxembourg (88%), Netherlands (87%), the UK (86%), Belgium (83%), Germany (72%) and Italy (67%) showing the highest values. In the case of Spain, it was 57%.

In the two regions under assessment, Spain and the UK, the heating demand for the analysis is calculated using non-renewable residential FEC values for heating [29], considering typical efficiencies of heating technologies by fuel, as defined in section 2.2.1, using Eqs. (1) and (2). The obtained monthly profiles of thermal heating demand values (MWh/month) are shown in Fig. 6, for Spain and the UK, respectively. It should be noted that the heating demand target for heating electrification was defined as a reference value of 10% current residential FEC associated with non-renewable energy for 2018 and 2019.

The selected thermal heating demand for heating electrification in Spain was 4822 GWh and 4768 GWh for 2018 and 2019. For the UK, it was 27,096 GWh and 26,815 GWh. These heat demand quantities suppose an additional electricity load considering HP efficiency and grid losses of 1489–1472 GWh/year in Spain and 8368–8281 GWh/year in the UK. This annual electricity volume represents 0.6% and 3.0% of existing annual electricity consumption for Spain and the UK, respectively.

3.1.2. Electricity grid per country

Fig. 7 summarises the electricity context of Spain (Fig. 7a) and the

UK (Fig. 7b) in 2018.

Total net electricity generation in Spain was 263.8 TWh in 2018 (263.7 TWh in 2019), of which 37.2 was based on renewable energy sources (36.1% in 2019), mainly hydro (13.7%), wind (18.8%) and solar (4.6%). Fossil fuels represent 42.6% (natural gas, coal and oil), while 20.2% came from nuclear power stations. In the case of the UK, total net electricity generation was 317.4 TWh in 2018 (310.3 TWh in 2019), of which 24.4% was based on renewable energy sources (27.4% in 2019), mainly wind (17.9%), solar (4.0%) and hydro (2.4%). More than half (57.0%) came from combustible fuels (natural gas, coal and oil), while 18.6% came from nuclear.

The overlapping of daily profiles associated with power consumption, hourly average carbon intensity and hourly average marginal carbon intensity for the period under assessment (2018–2019) in Spain and the UK are illustrated in Fig. 8.

The results show high variability in power demand (Fig. 8a1-b1) and hourly average carbon intensity (Fig. 8a2-b2) throughout the year, with higher intra-day differences in the UK. The mean power demand of Spain and the UK, during this period, was 28,674 MW and 32,065 MW, respectively. These values ranged between 20,000 MW and 40,000 MW in Spain and between 20,000 MW and 50,000 MW in the UK.

The mean carbon intensity rate was 221 gCO<sub>2eq</sub>/kWh and 260 gCO<sub>2eq</sub>/kWh for Spain and the UK (Fig. 8a2-b2), respectively, considering both years (2018–2019). The curves show a notable intra-day difference in the case of the UK mainly due to the significant variability of electricity demand between daytime and night, while in Spain, hourly oscillations are less significant. Hourly average marginal average carbon intensity profiles in Fig. 8a3-b3 illustrate the marginal power capacity per region in response to additional load. These values were lower in the case of Spain, showing a mean value of 260 gCO<sub>2eq</sub>/kWh. The Spanish profile also reflects lower hourly marginal carbon intensities during the daytime, corresponding to a higher marginal renewable capacity in the grid during these hours. Regarding the UK, the hourly average marginal carbon intensity rate presents no significant

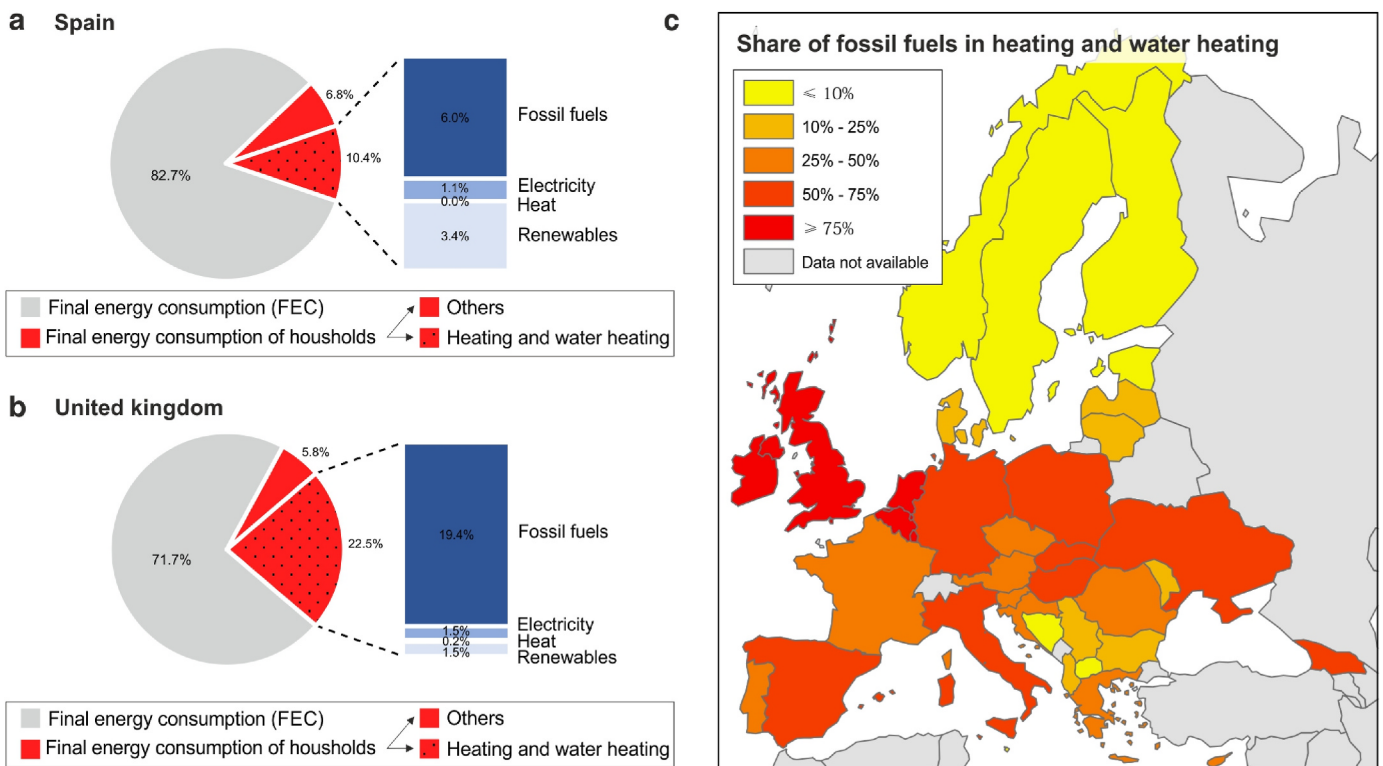


Fig. 5. The heating sector of households in Spain (a) and the UK (b) in 2018. Share of fossil fuels in the heating sector in Europe (c) in 2018. Data source: Eurostat [29].

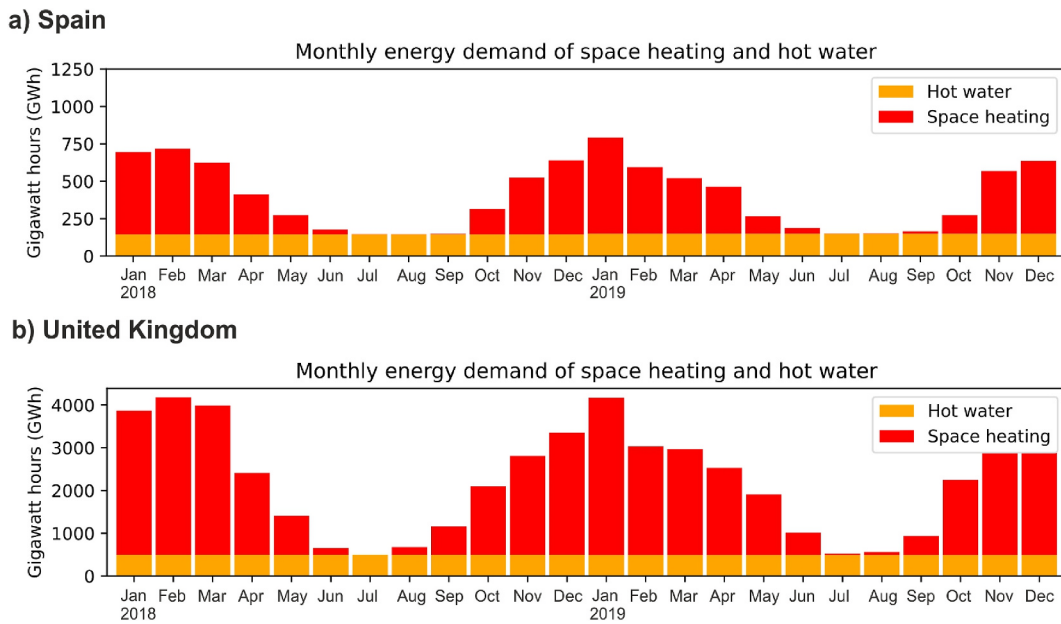


Fig. 6. Thermal heating demand profile corresponding to 10% of current heating based on fossil fuels in Spain (a) and the UK (b).

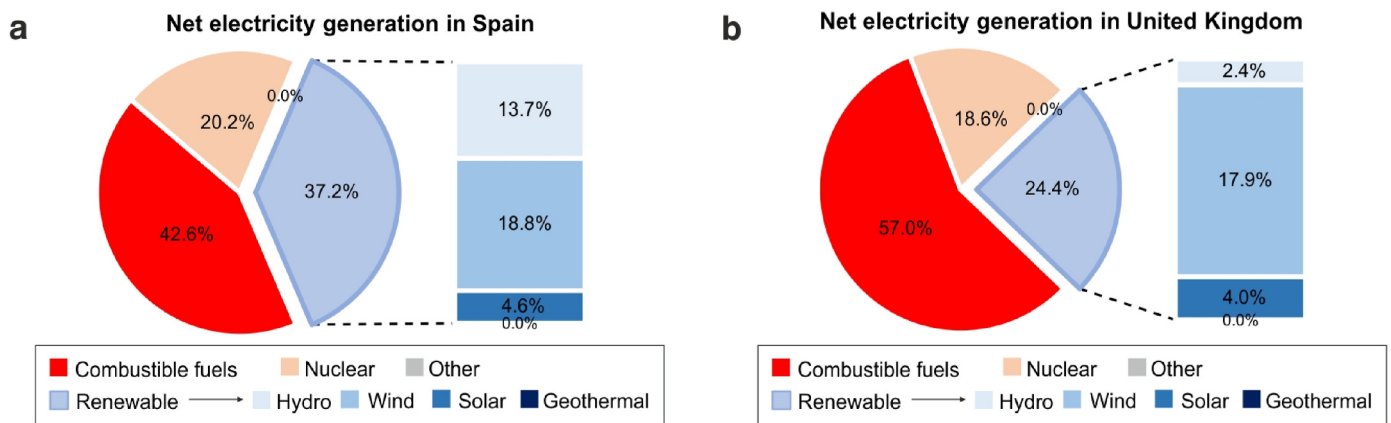


Fig. 7. Net electricity generation in Spain (a) and the UK (b) by source in 2018.

intra-day difference with a mean value of 532 gCO<sub>2eq</sub>/kWh, showing how marginal power capacity was based on non-renewable sources most of the time.

### 3.2. Analysis of output results: optimal heating electrification pathway per country

This section shows the results of heat storage for heating electrification through smart DR, shifting consumption from hours to days according to different TES capacities. The analysis is carried out using data for 2018 and 2019. The load for heating electrification was defined as a short-term reference target of 10% of non-renewable residential FEC for heating per country, according to existing data in Eurostat [29]. This fraction involves current FEC for heating based on solid fossil fuels, natural gas and oil and petroleum products. This additional energy volume for heating only represents 0.6% and 3.0% of annual electricity consumption for Spain and the UK, respectively. However, the hourly power intensity can be considerable since it is heterogeneously distributed throughout time, with maximum power capacity required during winter.

#### 3.2.1. Electricity load of different demand scenarios

Heating electrification is evaluated through a parametric analysis comprising ten scenarios (S1-10). An example of the parametric analysis through different load shifting strategies for 15 days of January 2019 is illustrated in Figs. 9 and 10 for Spain and the UK, respectively.

Figs. 9a and 10a show the hourly power consumption mix by technology and its associated average carbon intensity rate (BCI, gCO<sub>2eq</sub>/kWh). Average marginal carbon intensity (MCI) associated with marginal power capacity is also shown in a grey dashed line. The energy consumption mix considers imports and the additional wind generation introduced in the numerical model.

In Spain (Fig. 9a), the value of average baseline carbon intensity is more stable (between 200 and 300 gCO<sub>2eq</sub>/kWh) compared to the UK (Fig. 10a), where the value goes from 100 to 400 gCO<sub>2eq</sub>/kWh with sharper changes. The illustrated power consumption mix by region in Figs. 9a and 10a shows how nuclear generation is maintained almost constantly, with higher carbon emissions rates associated with higher power production linked to combustible fuels. Moreover, it can be observed how average marginal carbon intensity is always higher than the average value since it is mainly based on combustible fuels.

Figs. 9b and 10b illustrate the different scenarios for heating electrification, where the red area represents power consumption for

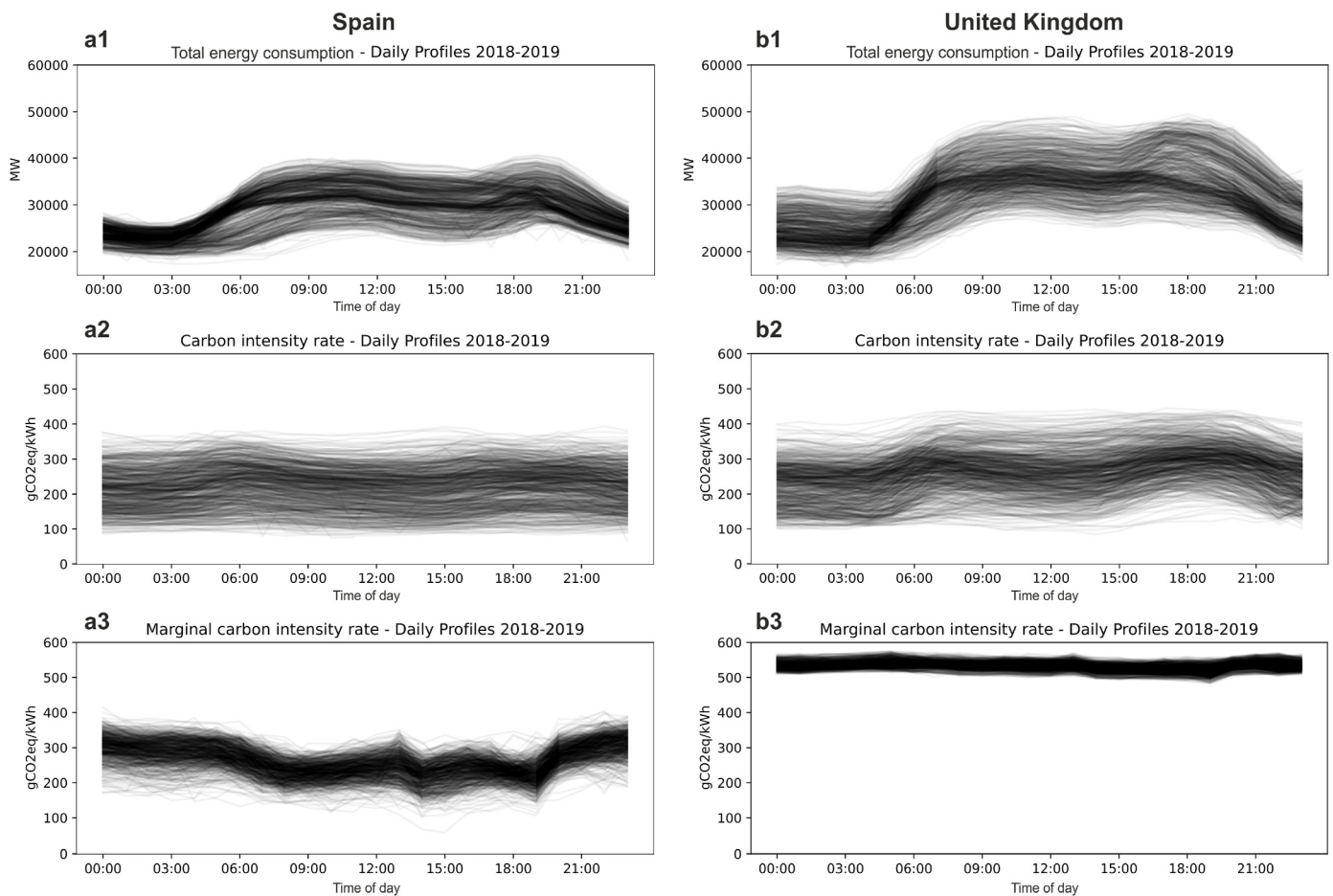


**Fig. 8.** Overlapping of daily profiles generated of Spain (a) and the UK (b) in 2018–2019 for power consumption (a1-b1), hourly average carbon intensity (a2-b2), and hourly average marginal carbon intensity (a3-b3).

heating, previously defined as  $LOAD_{s,h}$  (MW). They also include the average baseline carbon intensity rate (BCI, black dashed line) and the average updated carbon intensity rate (UCI, blue dashed line). The load shifting per scenario was calculated using average baseline carbon intensity (BCI) as a penalty signal, previously defined in Eq. (4). The UCI rate is lightly modified per scenario compared to BCI since it includes marginal power capacity for the additional electricity load for heating.

S1 and S2 show the two baseline scenarios without heat storage, with and without improving energy efficiency in buildings, respectively. They are responsible for an additional maximum power demand of 512 MW and 439 MW in Spain, and 2777 MW and 2337 MW in the UK. These values, associated with a 10% heating electrification scenario, represent a peak grid capacity increase by 1.2–1.1% and 4.6–3.9% in Spain and the UK, respectively.

For hourly DR scenarios S3–S6, additional maximum power demands between 395 MW and 513 MW in Spain and between 2063 MW and 2769 MW in the UK are observed. Finally, for daily DR scenarios S7–S10, additional maximum power demands between 532 MW and 552 MW in Spain and between 2886 MW and 3004 MW in the UK are observed.

The different electrification alternatives of heating modify the UCI rate per scenario, increasing it during consumption periods. UCI is calculated according to the additional hourly electricity load per scenario and marginal generation capacity. At first glance, in Fig. 9b in Spain, no differences are appreciable between the baseline and the updated value. This is produced due to the low additional load in this region. Contrastingly, in the UK (Fig. 10b), it can be appreciated a shift in the UCI rate per scenario during consumption periods (red blocks). This is produced because the UK has higher heating demand and most

marginal power capacity is mainly based on combustible fuels.

### 3.2.2. The influence of additional load on required power capacity

The influence of load shifting scenarios on required power capacity per region is evaluated in Fig. 11, which illustrates the load duration curve (baseline) and the additional power required in percentage (%) for Spain (Fig. 11a) and the UK (Fig. 11b). The load duration curve illustrates the relationship between generating capacity requirements and capacity utilization per scenario.

The results show how Spain’s 10% electrification pathway does not pose a significant challenge for the grid. Even baseline scenarios (S1 and S2) only increase power capacity by 1.2% (0.8% considering the 99th percentile). However, in the UK, the 10% electrification pathway under an uncoordinated scenario (S1) can increase the required power capacity by more than 4.6% (4.2% considering the 99th percentile). Even in scenario 2, following an energy efficiency pathway of 20%, the required capacity is increased by 3.9% (with the 99th percentile being 3.53%).

In the highly gas-dependent context of the UK, the analysis of different load shifting strategies highlights how the implementation of heat storage for 2 and 4 demand hours (S3 and S4) decreases the 99th percentile of additional power capacity to 3.15%. Optimal shifting capacities were found for 12 and 24 h (S6 and S7), reducing the 99th percentile of additional power capacity to 2.22% and 2.11%, respectively. These optimal scenarios represent a reduction of additional power capacity by 47% and 49% compared to S1, respectively, and by 37% and 40% compared to S2. Finally, no additional benefits for power capacity were found using daily DR strategies (S7–S10), shifting

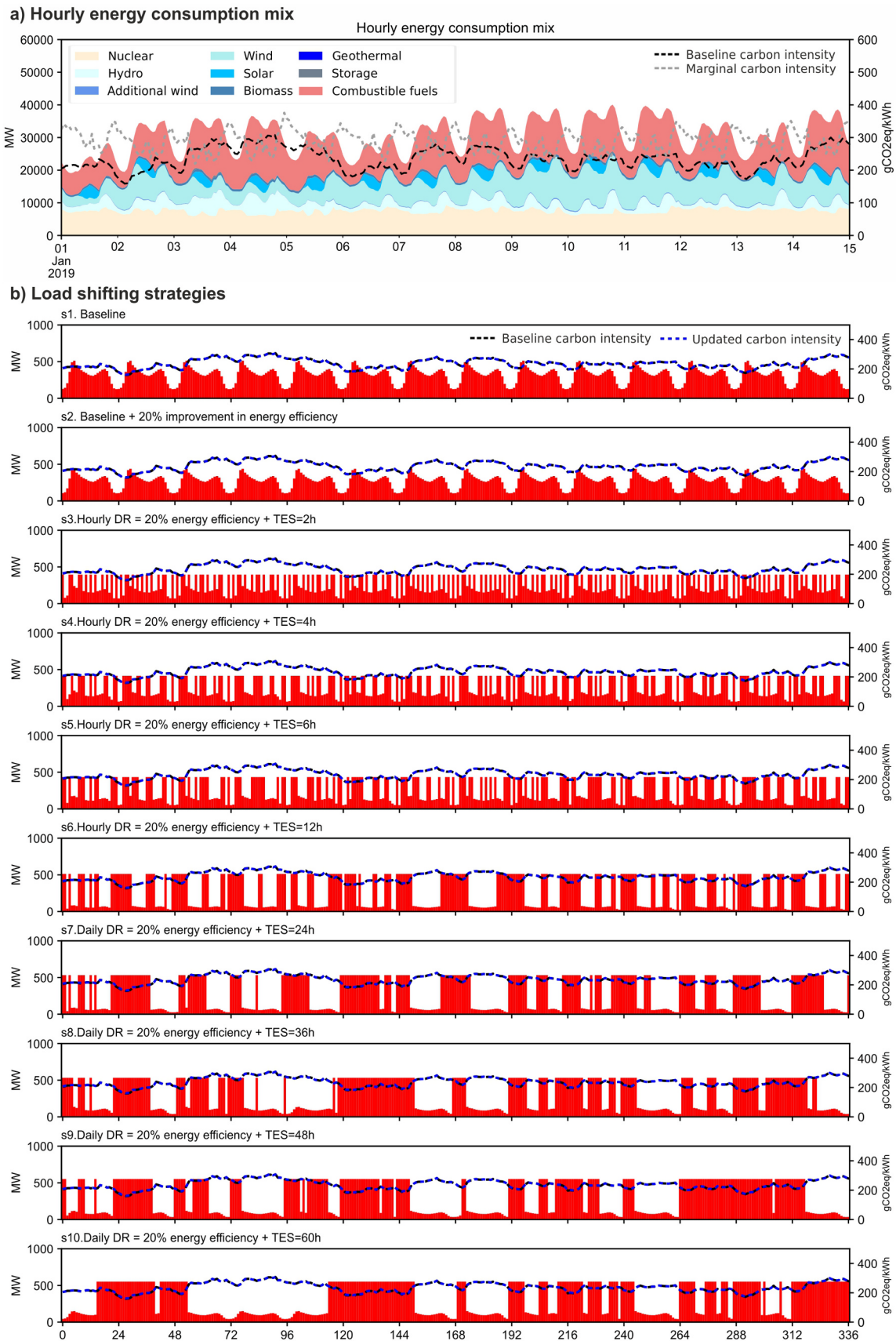
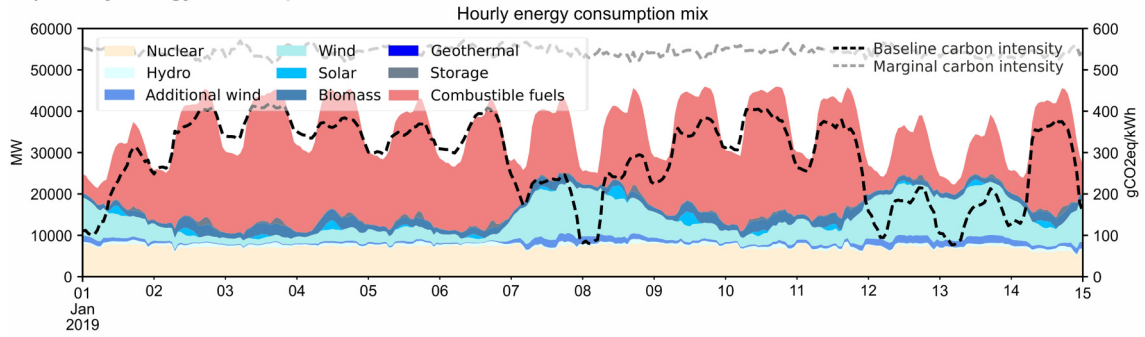
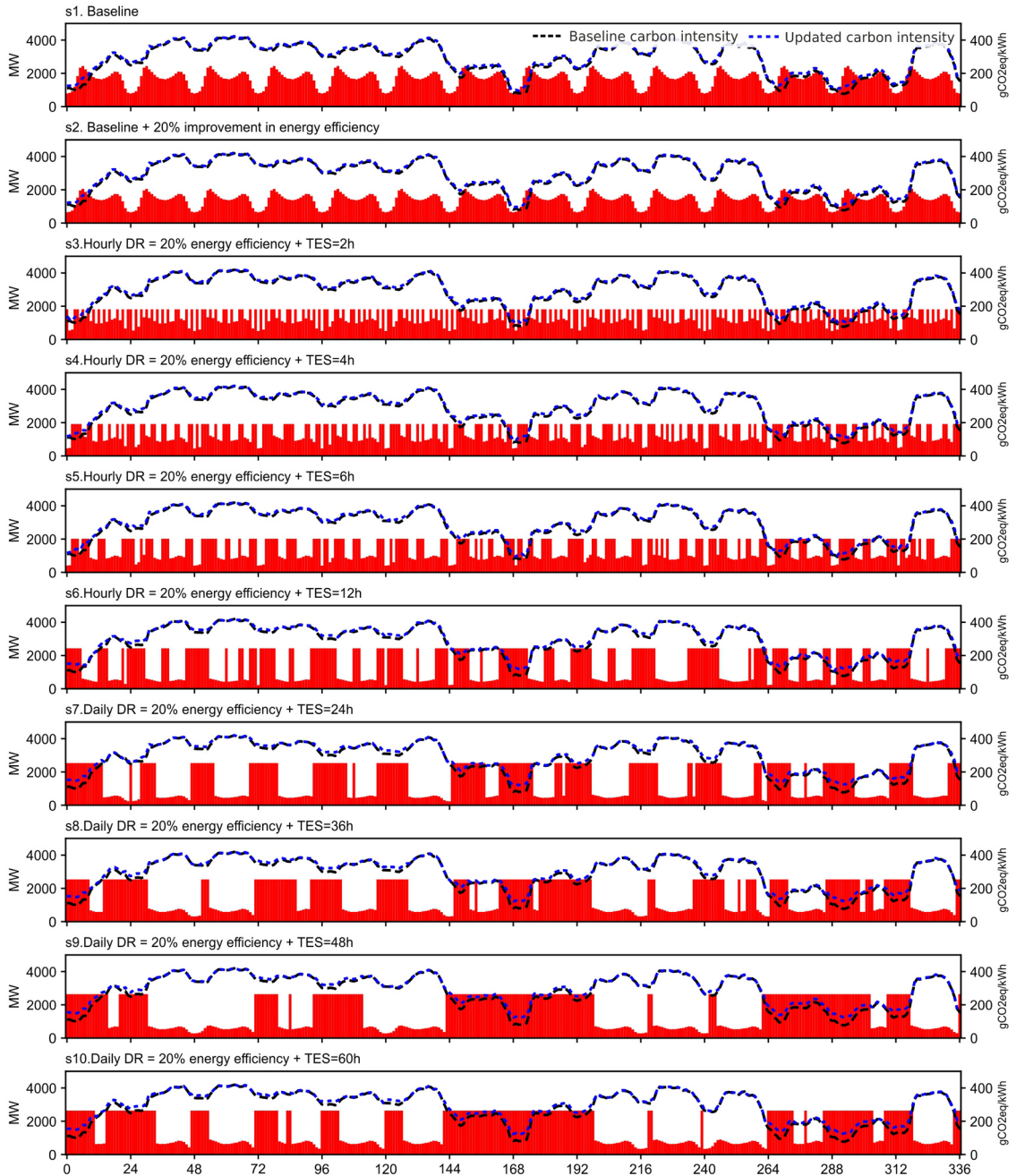


Fig. 9. Example of load shifting per each DR scenario in Spain during 15 days from January 01, 2019.

**a) Hourly energy consumption mix**



**b) Load shifting strategies**



**Fig. 10.** Example of load shifting per DR scenario in the UK during 15 days from January 01, 2019.

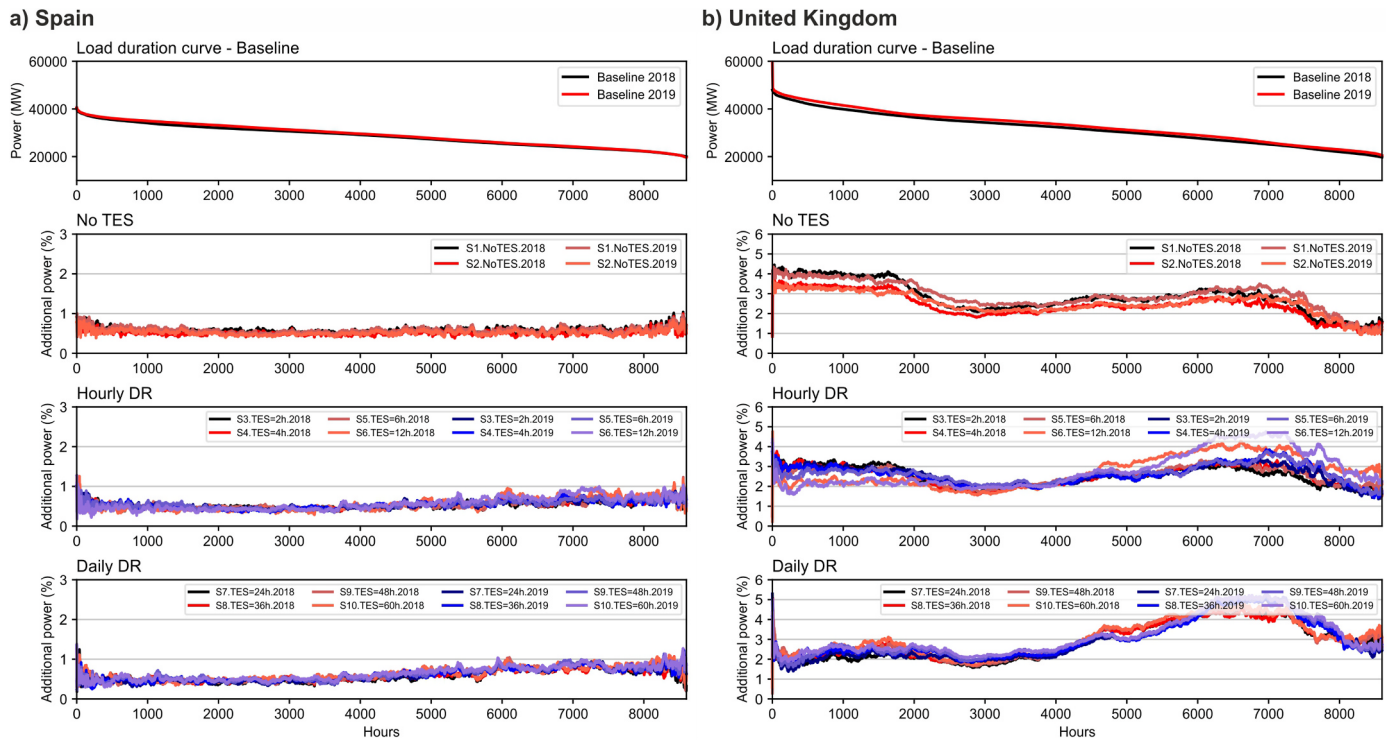


Fig. 11. Modification of power duration curve per scenario in Spain (a) and the UK (b).

consumption from 24 h to 60 h.

It can be observed how simulated DR scenarios result in higher peak demand than the baseline scenario during a few hours per year. This effect has been neglected, evaluating the peak power demand using the 99th percentile. These peak hours may be related to the use of BCI as a penalty signal since BCI is directly related to existing carbon emissions, not informing about peak consumption periods. In future scenarios, MCI may provide more useful information for load shifting to overcome this problem. However, MCI was not considered in this study due to the fact that it is almost constant with the current fossil-based marginal generation.

In comparison with previous studies on heat electrification in the UK, the results show conservative baseline projections. Love et al. [10] found

that peak grid demand may increase by 3.75 GW (7%) with 10% of households installing heat pumps. Our model shows how 10% of households may increase peak grid demand by approximately 2.5 GW (4.60%). The different results are likely explained through the differences in the analytical methods: the study of Love et al. [10] is based on accurate consumption data with peak consumption events; and the proposed numerical model does not consider peak consumption events since it was calculated using a normalised average heating demand profile (see Fig. 2).

### 3.2.3. GHG emissions per scenario

The environmental performance of different heating electrification scenarios per region is summarised in Fig. 12. Fig. 12a1-b1 shows the

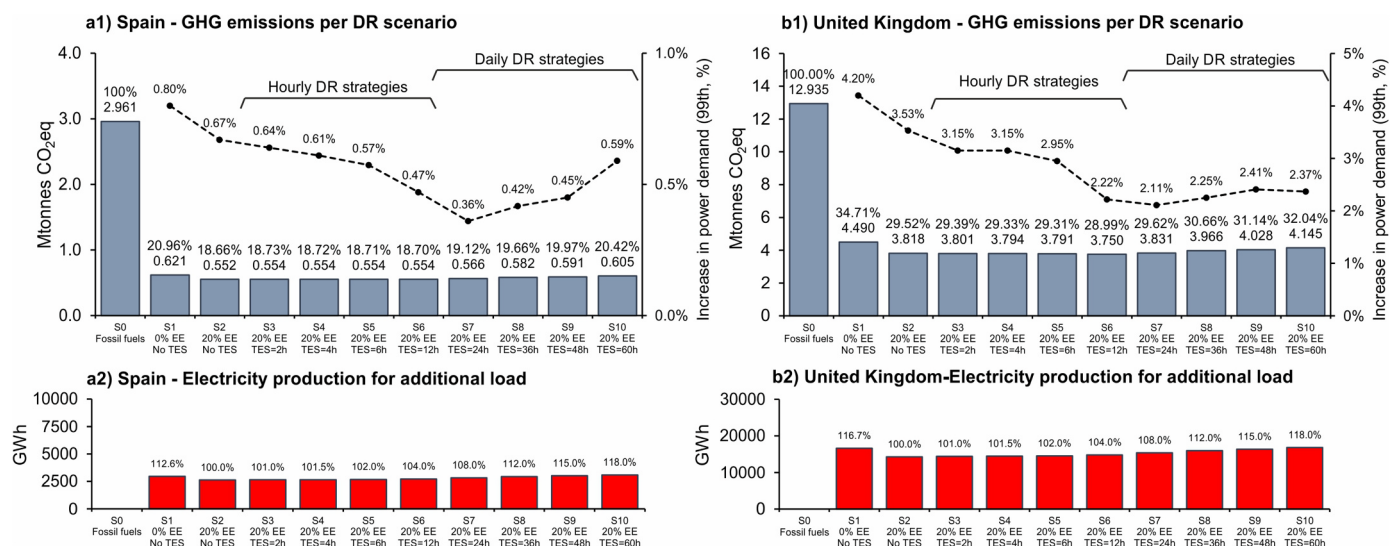


Fig. 12. GHG emissions and increase in power demand per load shifting scenario (1), and electricity consumption for the additional load in comparison with S2 (2). a, Spain. b, the UK.

impact of GHG emissions reduction considering marginal power capacity per scenario (left y-axis), with a black dashed line showing the 99th percentile of the increase in power capacity per scenario (right y-axis). S0 represents the reference GHG emissions scenario associated with evaluated heating demand based on fossil fuels. Moreover, Fig. 12a2-b2 provides the reference final electricity consumption associated with each scenario in comparison with S2.

The results show how heating electrification under direct electrification scenarios without TES for DR (S1 and S2) can reduce GHG impact by 79.0–81.3% and 65.3–70.5% for Spain and the UK, respectively. However, these electrification scenarios can negatively affect the electricity grid due to the increased power capacity required, as illustrated in Fig. 12a1-b1 (dashed line). Considering the environmental performance of S2 as a reference, the evaluated DR strategies for effective load shifting show limited, and even negative, benefits. This effect is mainly associated with increased energy consumption by scenario and current marginal power capacity based mainly on fossil fuels.

In the case of Spain, there is not much difference in carbon emissions by scenario. The lowest GHG emissions value was found to be S6, with a TES capacity of 12 demand hours (Fig. 12a1), and very similar to both S4 and S3. However, even this lowest value was found to be higher than reference scenario S2 by 0.21% due to increased energy consumption and marginal power availability.

In the case of the UK, the lowest GHG emission scenario was also found to be S6. This optimal DR was able to reduce carbon emissions by 1.8% in comparison with reference scenario S2 (Fig. 12b1), equivalent to an additional saving potential of 2.6 ktonnes CO<sub>2eq</sub> per year. Higher GHG emissions were found through shorter DR strategies (S3–S5). Moreover, it should be noted that in both countries, higher shifting capacities than 12 h (from S7 to S10) did not provide additional GHG reductions. Despite higher energy consumption during lower carbon intensity hours, the increase in electricity demand associated with thermal losses worsens environmental performance.

### 3.3. Policy implications

The results demonstrate the importance of exploring the implementation of DR strategies beyond the shifting capacity of 4 h in highly gas-dependent countries, such as the UK. In the case of the UK, 12 h of heat storage capacity for DR was able to reduce additional peak power capacity by 37% and mitigate GHG emissions by 1.8% in comparison with the baseline scenario S2. In the future, with the increase in the contribution of renewables to marginal generation, benefits will be greater and even higher shifting capacities may be of interest.

These findings highlight the added benefits that can come from the coupling of two heat decarbonisation measures: demand reduction and heat storage. Practical considerations that should be considered from these findings include addressing incumbent heating electrical systems, mainly driven by existing heating configurations and capital cost. For example, the most common efficient electrical heating system in the UK is an air-source heat pump (ASHP) using radiators, responsible for more than 82% of cases [10,36]. Supporting policies need to be designed to reduce capital costs to ensure the broad deployment of synergies between demand reduction and heating electrification with the required energy flexibility capability.

### 3.4. Limitations of the study

The scope of this work is limited to the residential sector and short-term targets since it is based on the existing performance of the energy grid and residential heating demand patterns. The method used to achieve hourly heating demand patterns is based on annual national data and monthly HDD to scale normalised national demand patterns. Thus, this method will likely involve a slight underestimate of instantaneous peak power demand. These assumptions were defined to ensure greater replicability of the modelling approach across other regions

where higher resolution data are unavailable. Additionally, the performance of TES technology associated with each load shifting scenario was defined according to the results provided by previous studies. It should be considered that more efficient TES alternatives with reduced heat losses could provide additional benefits to those reported in this study, particularly in the most prolonged shifting capacity scenarios. Such efficiency improvements could further mitigate carbon emissions and peak power demand but may require higher investment costs. With regards to marginal emissions, this study only considers a small deviation away from the existing generation mix, which is not expected to have a significant impact, if any, on the marginal emissions of the system. As renewable energy generation increases to the point where marginal emissions are changed, the environmental benefits of DR with TES should become even more apparent. Finally, reported findings are derived for two specific countries, Spain and the UK, based on existing generation technologies. Additional studies should be carried out to extend these conclusions to other regions and future scenarios.

## 4. Conclusions

This research proposes an energy modelling approach using national data to identify, country by country, the optimal heat storage capacity that should be promoted to support residential heating electrification through demand-side response (DR) to decrease additional peak power capacity and maximise carbon reductions. The model assesses the optimal shifting of heat pump operation according to different heat storage capacities in buildings, which are defined in relation to the time (in hours) in which the heating demand can be provided directly from the heat battery, without heat pump operation. Two baseline scenarios without heat storage were defined. The first involves direct electrification only (scenario S1), while the second considers electrification alongside a demand reduction of 20% due to improvements in energy efficiency in buildings (S2). Eight load shifting scenarios for heating electrification through different thermal energy storage (TES) capacities were evaluated, all considering the 20% demand reduction similar to S2. These load shifting scenarios are also compared with a reference scenario (S0), with heating currently based on fossil fuels. The method was applied to two countries, Spain and the UK, characterised by different existing non-renewable heating demands, power demand profiles and generation mix. A short-term electrification target of 10% of existing non-renewable residential final energy consumption (FEC) for heating per country was considered. Based on the results, the following conclusions are drawn:

The results show how heating electrification under scenarios without DR (S1 and S2) can reduce associated greenhouse gas (GHG) emissions by 79.0–81.3% and 65.3–70.5% for Spain and the UK, respectively. However, these electrification scenarios negatively affect the electricity grid due to the increase in peak power demand: up to 1.2% in Spain (0.8% considering the 99th percentile) and up to 4.6% in the UK (4.2% considering the 99th percentile).

The optimal TES capacity for smart DR is found on the order of 12 and 24 h of heating demand in both countries (S6 and S7). These scenarios reduce additional power capacity by 30–46% and 37–40% for Spain and the UK, respectively, in comparison with scenario S2 without DR.

The best environmental performance with lower peak capacity is found in scenario S6, with a TES capacity of 12 h of heating demand. In this scenario, GHG emissions increase by 0.21% in Spain and decrease by 1.78% in the UK in comparison with scenario S2. In comparison with the non-renewable heating scenario S0, this scenario S6 reduced associated carbon emissions by 81% and 71% for both countries, respectively. These low environmental benefits are associated with higher energy consumption in DR scenarios and marginal generation mainly based on fossil fuels.

It is also found that load shifting capability below 4 h presents limited benefits, reducing additional peak power capacity by

approximately 10%. Moreover, a higher shifting capacity than 24 h does not provide any additional benefits. Despite higher energy consumption during lower carbon intensity hours, the increase in electricity demand associated with thermal losses worsens environmental performance overall.

It should be highlighted that this evaluation is associated with marginal power capacity mainly based on fossil fuels. In the future, average marginal carbon intensity will decrease, involving additional implications to promote heat storage.

The findings highlight the importance of heat storage integration with heating decarbonisation targets, particularly in highly gas-dependent regions. Future regulations should promote these energy flexibility requirements in future heating technologies to help transform the power system, accommodate more renewable energy, and eliminate network reinforcement. This top-down energy modelling approach, available on GitHub (<https://github.com/lizanafj/national-data-based-energy-modelling>), is open and adaptable to different contexts and requirements using easily accessible data from the reported data sources.

**Declaration of competing interest**

The authors declare that they have no known competing financial

interests or personal relationships that could have appeared to influence the work reported in this paper.

**Data availability**

Data will be made available on request.

**Acknowledgements**

The authors gratefully acknowledge the financial support via a Juan de la Cierva Postdoctoral Fellowship granted to J. L. (FJC2019-039480-I) from the Spanish Ministry of Science and Innovation; and a PhD Fellowship granted to N. A. (PRE2018-085866) from the Spanish Ministry of Education, Culture and Sport. The research was also supported by the European Union’s Horizon 2020 research and innovation programme under the Marie Skłodowska-Curie grant agreement No 101023241. We are thankful for Tomorrow ([www.tmrow.com](http://www.tmrow.com)), who has provided the data used in this study.

**Appendix A**

Table 1a summarises the results obtained per region and scenario involving the electrification of 10% heating currently based on fossil fuels.

**Table 1a**  
Summary of results per region and scenario.

|   | S0<br>Fossil<br>fuels | S1<br>No TES | S2<br>20% EE<br>No TES | S3<br>20% EE<br>TES = 2 h | S4<br>20% EE<br>TES = 4 h | S5<br>20% EE<br>TES = 6 h | S6<br>20% EE<br>TES = 12 h | S7<br>20% EE<br>TES = 24 h | S8<br>20% EE<br>TES = 36 h | S9<br>20% EE<br>TES = 48 h | S10<br>20% EE<br>TES = 60 h |
|---|-----------------------|--------------|------------------------|---------------------------|---------------------------|---------------------------|----------------------------|----------------------------|----------------------------|----------------------------|-----------------------------|
| <b>a.Spain</b>  |                       |              |                        |                           |                           |                           |                            |                            |                            |                            |                             |
| <b>GHG emissions</b>  |                       |              |                        |                           |                           |                           |                            |                            |                            |                            |                             |
| GHG emissions (Mtonnes CO <sub>2</sub> eq)  | 2.961                 | 0.621        | 0.552                  | 0.554                     | 0.554                     | 0.554                     | 0.554                      | 0.566                      | 0.582                      | 0.591                      | 0.605                       |
| GHG emissions in comparison with S0 (%)   | 100%                  | 20.96%       | 18.66%                 | 18.73%                    | 18.72%                    | 18.71%                    | <b>18.70%</b>              | 19.12%                     | 19.66%                     | 19.97%                     | 20.42%                      |
| Marginal GHG emissions (considering only marginal power) (Mtonnes CO <sub>2</sub> eq) | 2.961                 | 0.752        | 0.668                  | 0.685                     | 0.690                     | 0.693                     | 0.706                      | 0.729                      | 0.753                      | 0.770                      | 0.789                       |
| <b>Power demand</b>   |                       |              |                        |                           |                           |                           |                            |                            |                            |                            |                             |
| Maximum power demand of the additional heating load (MW)                              |                       | 512          | 439                    | 395                       | 414                       | 434                       | 513                        | 532                        | 533                        | 552                        | 552                         |
| Maximum power demand of total consumption (MW)  |                       | 41,082       | 41,028                 | 41,105                    | 41,125                    | 41,123                    | 41,202                     | 40,890                     | 41,221                     | 40,910                     | 41,241                      |
| 99th percentile of the power demand of total consumption (99th percentile, MW)        |                       | 38,387       | 38,337                 | 38,329                    | 38,317                    | 38,348                    | 38,265                     | 38,222                     | 38,325                     | 38,256                     | 38,309                      |
| Increase in maximum power demand (99th percentile, MW)                                |                       | 304          | 253                    | 245                       | 233                       | 220                       | 181                        | 138                        | 160                        | 172                        | 225                         |
| Increase in maximum power demand (99th percentile, %)                                 |                       | 0.80%        | 0.67%                  | 0.64%                     | 0.61%                     | 0.57%                     | 0.47%                      | <b>0.36%</b>               | 0.42%                      | 0.45%                      | 0.59%                       |
| <b>Electricity consumption</b>  |                       |              |                        |                           |                           |                           |                            |                            |                            |                            |                             |
| Additional electricity consumption for heating (GWh)                                  |                       | 2953         | 2621                   | 2647                      | 2660                      | 2673                      | 2726                       | 2831                       | 2936                       | 3014                       | 3093                        |

(continued on next page)



Table 1a (continued)

|   | S0           | S1     | S2               | S3                  | S4                  | S5                  | S6                   | S7                   | S8                   | S9                   | S10                  |
|---|--------------|--------|------------------|---------------------|---------------------|---------------------|----------------------|----------------------|----------------------|----------------------|----------------------|
|   | Fossil fuels | No TES | 20% EE<br>No TES | 20% EE<br>TES = 2 h | 20% EE<br>TES = 4 h | 20% EE<br>TES = 6 h | 20% EE<br>TES = 12 h | 20% EE<br>TES = 24 h | 20% EE<br>TES = 36 h | 20% EE<br>TES = 48 h | 20% EE<br>TES = 60 h |
| <b>b. the United Kingdom</b>  |              |        |                  |                     |                     |                     |                      |                      |                      |                      |                      |
| <b>GHG emissions</b>  |              |        |                  |                     |                     |                     |                      |                      |                      |                      |                      |
| GHG emissions (Mtonnes CO <sub>2</sub> eq)  | 12.935       | 4.490  | 3.818            | 3.801               | 3.794               | 3.791               | 3.750                | 3.831                | 3.966                | 4.028                | 4.145                |
| GHG emissions in comparison with S0 (%)   | 100%         | 34.71% | 29.52%           | 29.39%              | 29.33%              | 29.31%              | <b>28.99%</b>        | 29.62%               | 30.66%               | 31.14%               | 32.04%               |
| Marginal GHG emissions (considering only marginal power) (Mtonnes CO <sub>2</sub> eq) | 12.935       | 8.912  | 7.634            | 7.711               | 7.754               | 7.797               | 7.959                | 8.270                | 8.569                | 8.798                | 9.025                |
| <b>Power demand</b>   |              |        |                  |                     |                     |                     |                      |                      |                      |                      |                      |
| Maximum power demand of the additional heating load (MW)                              |              | 2777   | 2337             | 2063                | 2181                | 2298                | 2769                 | 2886                 | 2886                 | 3003                 | 3004                 |
| Maximum power demand of total consumption (MW)  |              | 59,834 | 59,788           | 59,597              | 59,561              | 59,936              | 59,424               | 60,104               | 60,104               | 59,457               | 60,137               |
| 99th percentile of the power demand of total consumption (99th percentile, MW)        |              | 48,167 | 47,857           | 47,680              | 47,677              | 47,586              | 47,251               | 47,197               | 47,262               | 47,338               | 47,320               |
| Increase in maximum power demand (99th percentile, MW)                                |              | 1943   | 1634             | 1457                | 1454                | 1362                | 1027                 | 973                  | 1038                 | 1114                 | 1096                 |
| Increase in maximum power demand (99th percentile, %)                                 |              | 4.20%  | 3.53%            | 3.15%               | 3.15%               | 2.95%               | 2.22%                | <b>2.11%</b>         | 2.25%                | 2.41%                | 2.37%                |
| <b>Electricity consumption</b>  |              |        |                  |                     |                     |                     |                      |                      |                      |                      |                      |
| Additional electricity consumption for heating (GWh)                                  |              | 16,614 | 14,237           | 14,380              | 14,451              | 14,520              | 14,809               | 15,379               | 15,947               | 16,376               | 16,803               |

## References

- [1] IPCC. Climate change 2014: synthesis report, contribution of working groups I, II and III to the fifth assessment report of the intergovernmental Panel on climate change. Geneva, Switzerland: IPCC; 2014. [https://doi.org/10.1016/S0022-0248\(00\)00575-3](https://doi.org/10.1016/S0022-0248(00)00575-3).
- [2] The heat is on. Nat Energy 2016;1:16193. <https://doi.org/10.1038/nenergy.2016.193>.
- [3] IRENA. Innovation Outlook. Thermal energy storage. 2020.
- [4] Cabeza LF, de Gracia A, Zsembinszki G, Borri E. Perspectives on thermal energy storage research. Energy 2021;231:120943. <https://doi.org/10.1016/j.energy.2021.120943>.
- [5] International Energy Agency. Transition to sustainable buildings. Strategies and opportunities to 2050. OECD/IEA; 2013. <https://doi.org/10.1787/9789264202955-en>.
- [6] Scarlat N, Prussi M, Padella M. Quantification of the carbon intensity of electricity produced and used in Europe. Appl Energy 2022;305:117901. <https://doi.org/10.1016/j.apenergy.2021.117901>.
- [7] Gross R, Hanna R. Path dependency in provision of domestic heating. Nat Energy 2019;4:358–64. <https://doi.org/10.1038/s41560-019-0383-5>.
- [8] McKenna E, Thomson M. High-resolution stochastic integrated thermal-electrical domestic demand model. Appl Energy 2016;165:445–61. <https://doi.org/10.1016/j.apenergy.2015.12.089>.
- [9] Borge-Diez D, Icaza D, Trujillo-Cueva DF, Açıklalp E. Renewable energy driven heat pumps decarbonization potential in existing residential buildings: roadmap and case study of Spain. Energy 2022;247. <https://doi.org/10.1016/j.energy.2022.123481>.
- [10] Love J, Smith AZP, Watson S, Oikonomou E, Summerfield A, Gleeson C, et al. The addition of heat pump electricity load profiles to GB electricity demand: evidence from a heat pump field trial. Appl Energy 2017;204:332–42. <https://doi.org/10.1016/j.apenergy.2017.07.026>.
- [11] Watson SD, Lomas KJ, Buswell RA. Decarbonising domestic heating: what is the peak GB demand? Energy Pol 2019;126:533–44. <https://doi.org/10.1016/j.enpol.2018.11.001>.
- [12] Watson SD, Lomas KJ, Buswell RA. How will heat pumps alter national half-hourly heat demands? Empirical modelling based on GB field trials. Energy Build 2021; 238:110777. <https://doi.org/10.1016/j.enbuild.2021.110777>.
- [13] Mitchell C. Momentum is increasing towards a flexible electricity system based on renewables. Nat Energy 2016;1. <https://doi.org/10.1038/nenergy.2015.30>.
- [14] Langevin J, Harris CB, Satre-Meloy A, Chandra-Putra H, Speake A, Present E, et al. US building energy efficiency and flexibility as an electric grid resource. Joule 2021;5:2102–28. <https://doi.org/10.1016/j.joule.2021.06.002>.
- [15] Sandoval D, Goffin P, Leibundgut H. How low exergy buildings and distributed electricity storage can contribute to flexibility within the demand side. Appl Energy 2017;187:116–27. <https://doi.org/10.1016/j.apenergy.2016.11.026>.
- [16] Shimoda Y, Yamaguchi Y, Iwafune Y, Hidaka K, Meier A, Yagita Y, et al. Energy demand science for a decarbonized society in the context of the residential sector. Renew Sustain Energy Rev 2020;132:110051. <https://doi.org/10.1016/j.rser.2020.110051>.
- [17] IRENA. Demand-side flexibility for power sector transformation analytical brief demand-side flexibility for power sector transformation. International Renewable Energy Agency; 2019.
- [18] IRENA. Innovation Outlook. Smart charging for electric vehicles. International Renewable Energy Agency; 2019.
- [19] Edmunds C, Galloway S, Dixon J, Bukhsh W, Elders I. Hosting capacity assessment of heat pumps and optimised electric vehicle charging on low voltage networks. Appl Energy 2021;298:117093. <https://doi.org/10.1016/j.apenergy.2021.117093>.
- [20] Muratori M. Impact of uncoordinated plug-in electric vehicle charging on residential power demand. Nat Energy 2018;3:193–201. <https://doi.org/10.1038/s41560-017-0074-z>.
- [21] Lizana J, Friedrich D, Renaldi R, Chacartegui R. Energy flexible building through smart demand-side management and latent heat storage. Appl Energy 2018;230: 471–85. <https://doi.org/10.1016/j.apenergy.2018.08.065>.
- [22] Hedegaard K, Mathiesen BV, Lund H, Heiselberg P. Wind power integration using individual heat pumps - analysis of different heat storage options. Energy 2012;47: 284–93. <https://doi.org/10.1016/j.energy.2012.09.030>.
- [23] Hedegaard K, Balyk O. Energy system investment model incorporating heat pumps with thermal storage in buildings and buffer tanks. Energy 2013;63:356–65. <https://doi.org/10.1016/j.energy.2013.09.061>.
- [24] Heinen S, Turner W, Cradden L, McDermott F, O'Malley M. Electrification of residential space heating considering coincidental weather events and building

- thermal inertia: a system-wide planning analysis. *Energy* 2017;127:136–54. <https://doi.org/10.1016/j.energy.2017.03.102>.
- [25] ElectricityMap Database. Tomorrow. n.d. <https://app.electricitymap.org/map>. [Accessed 25 January 2021]. accessed.
- [26] Tranberg B, Corradi O, Lajoie B, Gibon T, Staffell I, Andresen GB. Real-time carbon accounting method for the European electricity markets. *Energy Strategy Rev* 2019;26. <https://doi.org/10.1016/j.esr.2019.100367>.
- [27] Leerbeck K, Bacher P, Junker RG, Goranović G, Corradi O, Ebrahimi R, et al. Short-term forecasting of CO<sub>2</sub> emission intensity in power grids by machine learning. *Appl Energy* 2020;277. <https://doi.org/10.1016/j.apenergy.2020.115527>.
- [28] Li H, Wang Z, Hong T, Piette MA. Energy flexibility of residential buildings: a systematic review of characterization and quantification methods and applications. *Adv Appl Energy* 2021;3:100054. <https://doi.org/10.1016/j.adapen.2021.100054>.
- [29] Eurostat. European statistics n.d. <https://ec.europa.eu/eurostat/web/main/home>. [Accessed 19 January 2020]. accessed
- [30] Government of the United Kingdom. Research and statistics in the UK. n.d. <https://www.gov.uk/search/research-and-statistics>. [Accessed 6 December 2021]. accessed.
- [31] Eurostat. Energy data - 2020 edition. Publications Office of the European Union; 2020.
- [32] Eurostat. Energy, transport and environment statistics. 2020 edition. Publications Office of the European Union; 2020.
- [33] Ruhnau O, Hirth L, Praktiknjo A. Time series of heat demand and heat pump efficiency for energy system modeling. *Sci Data* 2019;6:1–10. <https://doi.org/10.1038/s41597-019-0199-y>.
- [34] Ruhnau O, Muessel J. Update and extension of the When2Heat dataset. 2022.
- [35] Ruhnau O, Muessel J. When2Heat heating profiles. *Open Power System Data*; 2022.
- [36] Renewable heat premium payment scheme. 2014. <http://www.nidirect.gov.uk/index/information-and-services/environment-and-greener-living/energy-wise/energy-saving-grants/renewable-heat-grants/renewable-heat-premium-payment-rhpp.htm>. [Accessed 4 April 2022]. accessed.
- [37] Ippc. Annex II: metrics & methodology. *Climate change 2014: mitigation of climate change contribution of working group III to the fifth assessment report of the intergovernmental Panel on climate change*. 2014. p. 1281–328.
- [38] Ippc. Annex III: technology - specific cost and performance parameters. *Climate change 2014: mitigation of climate change contribution of working group III to the fifth assessment report of the intergovernmental Panel on climate change*. 2014. p. 1329–56. <https://doi.org/10.1017/cbo9781107415416.025>.
- [39] github. CO<sub>2</sub>eq parameters of ElectricityMap. n.d. [https://github.com/tmrowco/electricitymap-contrib/blob/master/config/co2eq\\_parameters.json](https://github.com/tmrowco/electricitymap-contrib/blob/master/config/co2eq_parameters.json). [Accessed 15 July 2021]. accessed.
- [40] Corradi O. Estimating the marginal carbon intensity of electricity with machine learning. ElectricityMap n.d. <https://electricitymap.org/blog/marginal-carbon-intensity-of-electricity-with-machine-learning/>. [Accessed 10 December 2021]. accessed
- [41] Lizana J, Chacartegui R, Barrios-Padura A, Ortiz C. Advanced low-carbon energy measures based on thermal energy storage in buildings: a review. *Renew Sustain Energy Rev* 2018;82:3705–49. <https://doi.org/10.1016/j.rser.2017.10.093>.
- [42] Arteconi A, Hewitt NJ, Polonara F. Domestic demand-side management (DSM): role of heat pumps and thermal energy storage (TES) systems. *Appl Therm Eng* 2013;51:155–65. <https://doi.org/10.1016/j.applthermaleng.2012.09.023>.
- [43] Jin X, Wu F, Xu T, Huang G, Wu H, Zhou X, et al. Experimental investigation of the novel melting point modified Phase-Change material for heat pump latent heat thermal energy storage application. *Energy* 2021;216:119191. <https://doi.org/10.1016/j.energy.2020.119191>.
- [44] Lizana J, Chacartegui R, Barrios-Padura A, Valverde JM. Advances in thermal energy storage materials and their applications towards zero energy buildings: a critical review. *Appl Energy* 2017;203:219–39. <https://doi.org/10.1016/j.apenergy.2017.06.008>.
- [45] Lizana J, Serrano-Jimenez A, Ortiz C, Becerra JA, Chacartegui R. Energy assessment method towards low-carbon energy schools. *Energy* 2018;159:310–26. <https://doi.org/10.1016/j.energy.2018.06.147>.